Journal of the American Heart Association

ORIGINAL RESEARCH

Age-Independent Cardiac Protection by Pharmacological Activation of Beclin-1 During Endotoxemia and Its Association With Energy Metabolic Reprograming in Myocardium—A Targeted Metabolomics Study

Matthew Kim, BS*; Azadeh Nikouee, PhD*; Raymond Zou; Di Ren, PhD; Zhibin He, PhD; Ji Li, PhD; Lu Wang, PhD; Danijel Djukovic, PhD; Daniel Raftery, PhD; Hayley Purcell, BS; Daniel Promislow, PhD; Yuxiao Sun, PhD; Mohammad Goodarzi, PhD; Qing-Jun Zhang, PhD; Zhi-Ping Liu, PhD; Qun Sophia Zang, PhD

BACKGROUND: We showed that Beclin-1-dependent autophagy protects the heart in young and adult mice that underwent endotoxemia. Herein, we compared the potential therapeutic effects of Beclin-1 activating peptide, TB-peptide, on endotoxemia-induced cardiac outcomes in young adult and aged mice. We further evaluated lipopolysaccharide (lipopolysaccharide)-induced and TB-peptide treatment-mediated alterations in myocardial metabolism.

METHODS AND RESULTS: C57BL/6J mice that were 10 weeks and 24 months old were challenged by lipopolysaccharide using doses at which cardiac dysfunction occurred. Following the treatment of TB-peptide or control vehicle, heart contractility, circulating cytokines, and myocardial autophagy were evaluated. We detected that TB-peptide boosted autophagy, attenuated cytokines, and improved cardiac performance in both young and aged mice during endotoxemia. A targeted metabolomics assay was designed to detect a pool of 361 known metabolites, of which 156 were detected in at least 1 of the heart tissue samples. Lipopolysaccharide-induced impairments were found in glucose and amino acid metabolisms in mice of all ages, and TB-peptide ameliorated these alterations. However, lipid metabolites were upregulated in the young group but moderately downregulated in the aged by lipopolysaccharide, suggesting an age-dependent response. TB-peptide mitigated lipopolysaccharide-mediated trend of lipids in the young mice but had little effect on the aged. (Study registration: Project DOI: https://doi.org/10.21228/M8K11W).

CONCLUSIONS: Pharmacological activation of Beclin-1 by TB-peptide is cardiac protective in both young and aged population during endotoxemia, suggest a therapeutic potential for sepsis-induced cardiomyopathy. Metabolomics analysis suggests that an age-independent protection by TB-peptide is associated with reprograming of energy production via glucose and amino acid metabolisms.

Key Words: autophagy ■ Beclin-1 ■ cardiac function ■ cardiac metabolism ■ endotoxemia ■ sepsis

Correspondence to: Qun Sophia Zang, PhD, Department of Surgery, Burn & Shock Trauma Research Institute, CTRE 321, Stritch School of Medicine, Loyola University Chicago Health Science Campus, 2160 S. 1st Ave, Maywood, IL 60153. Email: qzang@luc.edu

*M. Kim and A. Nikouee contributed equally.

Supplemental Material is available at https://www.ahajournals.org/doi/suppl/10.1161/JAHA.122.025310

For Sources of Funding and Disclosures, see page 24.

JAHA is available at: www.ahajournals.org/journal/jaha

CLINICAL PERSPECTIVE

What Is New?

- Using a mouse model of endotoxemia, we found that administration of a cell-permeable Beclin-1 activating peptide, TB-peptide, improves cardiac outcomes not only in young adult mice but also in aged mice in response to lipopolysaccharide-challenge.
- By a targeted metabolomics approach, we detected that, although lipopolysaccharide induces a drastic shifting of metabolic profiling in myocardium, TB-peptide reprograms energy production via glucose and amino acid metabolisms, suggesting a mechanism of action of this pharmacological agent.

What Are the Clinical Implications?

- Our data suggest that pharmacological Beclin-1 activating TB-peptide possesses a promising therapeutic value for sepsis-induced cardiomyopathy in different age groups.

Sepsis is a life-threatening condition of organ dysfunction caused by a deregulated host response to infection.[1] Despite improvements in antibiotic therapies and critical care techniques,[2] sepsis remains a leading cause of death in critical care units, and its reported incidence is still increasing.[3] Therefore, understanding the pathological mechanisms and exploring new therapeutic interventions for sepsis has become an urgent task.

Cardiomyopathy is an identified serious component of the multiorgan failure associated with sepsis.[4] Energy expenditure is a main regulatory element of cardiac contractility, and metabolism changes dynamically with physiological and pathological conditions. The normal heart is equipped with a remarkable degree of metabolic flexibility, whereby ATP is rapidly supplied via multiple substrates, such as fatty acids, carbohydrates, ketones, and amino acids (AAs), to meet the energy demand. Failing in cardiac performance is often associated with metabolic inflexibility, under which condition the heart loses the capability of using certain commonly used substrates. In sepsis models, this problem of metabolic inflexibility is apparent in the heart, as well as in other organs and circulating immune cells.[5–11] Current research in immunometabolism has revealed that disturbance in the energy metabolism of immune cells magnifies the adverse symptoms in sepsis.[12] However, in additional to inciting overwhelming inflammation, how the disturbance of metabolic homeostasis in immune cells and in other cell types leads to multiorgan failure, such as cardiomyopathy, remains unclear.

In the heart, mitochondria occupy about 30% of the cardiomyocyte volume.[13] Previous research in preclinical sepsis models elucidated that impairment in mitochondrial structure and function results in an overproduction of mitochondrial reactive oxygen species and a generation of mitochondria-derived danger-associated molecular patterns, inducing cardiac inflammation and functional deficiencies.[9,14–16] As the main source of energy production in the heart, mitochondria supply 90% of the total ATP via metabolism of glucose, AAs, and fatty acids. Therefore, deficiencies in mitochondria are likely the main cause for metabolic inflexibility in septic hearts. A comprehensive understanding of alterations in mitochondria and related metabolic reprograming will help to identify novel therapeutic targets and to develop effective strategies for improving clinical outcomes.

We recently investigated the role of autophagy, a self-survival lysosome-dependent process,[17] in the control of cardiac performance during endotoxemia.[18] We discovered that promoting autophagy via specific activation of Beclin-1, a universally expressed autophagy initiation factor,[19,20] improved cardiac contractility, protected mitochondria, and suppressed mitochondrial danger-associated molecular patterns in response to endotoxemia.[18] Accordingly, we further examined the potential therapeutic value of TB-peptide, a cell-permeable peptide that specifically activates Beclin-1, in sepsis animal models using young adult mice.[18,21,22] In the investigation summarized in this report, we further evaluated TB-peptide's effects on cardiac function of aged animals during endotoxemia. In addition, we applied a targeted metabolomics approach to compare how lipopolysaccharide alters metabolic profiling in the heart of young adult and aged mice and to examine whether TB-peptide reprograms cardiac metabolism in this animal model of endotoxemia.

METHODS

The data that support the findings of this study are available from the corresponding author upon reasonable request. The metabolomics analysis in this study is available at the National Institutes of Health Common Fund's National Metabolomics Data Repository website,[23] the Metabolomics Workbench (supported by National Institutes of Health grant U2C-DK119886), https://www.metabolomicsworkbench.org where it has been assigned Study ID ST002178. The data can be accessed directly via its Project DOI: https://doi.org/10.21228/M8K11W.

Experimental Animals

Wild-type C57BL/6 mice were obtained from Charles River laboratories (Wilmington, MA) and an in-campus

mouse breeding core facility at the University of Texas Southwestern Medical Center. All animals were conditioned in house for 5 to 6 days after arrival with commercial diet and tap water available ad libitum. Animal work described in this study was reviewed by and conducted under the oversight of the University of Texas Southwestern Medical Center Institutional Animal Care and Use Committee and conformed to the National Research Council's *Guide for the Care and Use of Laboratory Animals* when establishing animal research standards.

Endotoxemia was induced in young (10-week) and aged (24-week) male mice by lipopolysaccharide (lipopolysaccharide). Based on published results as well as observations in our laboratory, male and female mice showed significantly different susceptibility to systemic symptoms in sepsis models.[24] Thus, male but not female mice were chosen for the experiments presented in this report. lipopolysaccharide was administered intraperitoneally, and mice were weighed individually to determine the exact amount of lipopolysaccharide (MilliporeSigma, Burlington, MA; catalog number L3012) required to achieve the doses indicated in the figure legends. Sterile endotoxin-free PBS was used as a vehicle control in sham groups. In some experiments, TB-peptide, synthesized according to a published sequence[25] by NonoPep (Shanghai, China), was administered intraperitoneally at a dose of 16 mg/kg in 100 μL of PBS 30 minutes post lipopolysaccharide challenge.

Echocardiography

Transthoracic echocardiograms were recorded in sedated mice using Visualsonics Vevo 2100 small animal echocardiography machine. Views were taken in planes that approximated the parasternal short-axis view and the apical long-axis view in humans. The cardiac systolic and diastolic functions of randomly selected animals from each group were assessed using the previously described protocol.[18,26,27]

Preparation of Serum and Tissue Lysates

When animals were euthanized, blood was collected using BD vacutainer rapid serum tubes (BD Diagnostics, Franklin Lakes, NJ) followed by immediate centrifugation at 3000*g* for 15 minutes at 4 °C to isolate serum. The serum preparations were then allocated and stored at −80 °C until used. Tissues were harvested, washed in PBS, snap clamp frozen, and kept at −80 °C. Tissue lysates were prepared using tissue protein extraction reagent (Thermo Fisher Scientific, Rockford, IL; catalog number 78510). Protein concentrations were quantified using detergent compatible Bradford assay kit (Thermo Fisher Scientific, Rockford, IL; catalog number 23246).

Measurements of Cytokines by ELISA

Cytokine levels in serum were measured using Bio-Plex Mouse Cytokine Panel A 6-Plex (Bio-Rad, Hercules, CA; catalog number M6000007NY) according to vendor's instructions. Results were normalized by volume of serum samples or by the amount of protein in tissue lysate samples.

Measurement of Myocardial Lactate

The levels of lactate in heart tissue lysates were quantified by lactate assay kit (MilliporeSigma; Catalog Number MAK064) according to vendor's instructions. Results were normalized by the amount of protein in tissue lysate samples.

Western Blots

Procedures were performed according to established protocol.[18] Briefly, prepared SDS-PAGE protein samples were loaded to and run on 15% SDS-PAGE gels and transferred to polyvinylidene fluoride membranes. Membranes were blocked with 5% nonfat milk-PBS at room temperature for 1 hour and subsequently probed with antibody against LC3A/B (Cell Signaling, Danvers, MA; catalog number 4108). The membranes were then rinsed and incubated with corresponding horseradish peroxidase-conjugated antirabbit IgG (Bio-Rad, Hercules, CA; catalog number 170-6515). Antibody dilutions and incubation time were according to manufacturer's instructions. At the end, membranes were rinsed, and bound antibodies were detected by using SuperSignal West Pico Chemiluminescent Substrate (Thermo Scientific; catalog number 34077).

Targeted Liquid Chromatography–Mass Spectrometry Metabolite Analysis

(1) *Sample preparation*: aqueous metabolites were extracted using a methanol-based protein precipitation method as described previously.[28] Briefly, heart tissue samples were homogenized in cold water using zirconium oxide beads, methanol was added, and samples were vortexed and then stored for 30 minutes at −20 °C. Afterwards, samples were first sonicated in an ice bath for 10 minutes, centrifuged for 15 minutes at 18 000*g* and 4 °C, and then a fixed volume of supernatant was collected from each sample. Lastly, recovered supernatants were dried on a SpeedVac and reconstituted for liquid chromatography–mass spectrometry (LC–MS) analysis. Protein pallets that were left over from the sample prep were saved for bicinchoninic acid assay. (2) *LC–MS analysis*: samples were analyzed on a duplex-LC–MS system composed of 2 Shimadzu UPLC pumps, CTC Analytics PAL HTC-xt temperature-controlled auto-sampler, and AB Sciex 6500+ Triple Quadrupole MS equipped

with electrospray ionization source. UPLC pumps were connected to the auto-sampler in parallel and were able to perform 2 chromatography separations independently from each other. Each sample was injected twice on 2 identical analytical columns (Waters XBridge BEH Amide XP) performing separations in hydrophilic interaction liquid chromatography mode. While one column was performing separation and MS data acquisition in electrospray (+) ionization mode, the other column was getting equilibrated for sample injection, chromatography separation and MS data acquisition in electrospray(–) ionization mode. Each chromatography separation was 18 minutes (total analysis time per sample was 36 minutes). (3) *Data acquisition*: MS data acquisition was performed in multiple-reaction-monitoring mode. The whole LC–MS system was controlled using AB Sciex Analyst 1.6.3 software. Measured MS peaks were integrated using AB Sciex MultiQuant 3.0.3 software. In addition to the study samples, 2 sets of quality control (QC) samples were used to monitor the assay performance as well as data reproducibility. One QC was a pooled human serum sample used to monitor system performance and the other QC was pooled study samples and this QC was used to monitor data reproducibility. Isotope labeled compounds were used to monitor sample preparation and injection. Highly reproducible MS data were generated, having an average coefficient of variance among the metabolites of 5.6%. Data for each sample were normalized according to bicinchoninic acid-based quantification of total protein count.

Statistical Analysis

Analysis was carried out using R (version 4.0.2). The targeted metabolomics assay was designed to detect 361 metabolites and was conducted at the University of Washington's Nathan Shock Center of Excellence in the Biology of Aging and Northwest Metabolomics Research Center. A median normalization was performed to adjust the data so that samples had the same median value of the metabolite abundance post log2 transformation. Only metabolites with <20% missingness and a coefficient of variance <20% in the pooled sample QC data were considered in further analysis. Out of the possible 361 metabolites that the assay could detect, 161 metabolites passed these filtering criteria, which were included in the imputation step. We used a quantile regression approach for the imputation of left-censored missing data, which has been suggested as the favored imputation method for left-censored missing not at random data.[29] This was implemented in the R imputeLCMD package.

A linear model fit to the normalized metabolomic data using the Bioconductor limma package[30] was used to examine the treatment group difference within the same age group. The limma package uses empirical Bayes moderated statistics, which improves power by "borrowing strength" between metabolites to moderate the residual variance.[31] Metabolites with a false discovery rate of 10% were selected. Two-way or 3-way Venn diagrams were generated to identify common and unique metabolites among comparisons. Pathway analysis was performed by using Shiny GAM (integrated analysis of genes and metabolites) and Cytoscape software. Signaling networks were built on pathway clustering against the small molecule pathway database using MBRole 2.0 software.

RESULTS

TB-Peptide Provides Cardiac Protection in Both Young Adult and Aged Mice During Endotoxemia

Our previous research provided evidence that stimulating Beclin-1 dependent autophagy improves cardiac performance during endotoxemia in young adult mice, and thus TB-peptide holds a promising therapeutic potential for sepsis.[32] In this report, we examined whether TB-peptide exerts a similar protective effect on aged animals under the same condition. In our experimental setting, sham or lipopolysaccharide challenge was administered to groups of 24-month-old and 10-week-old mice at indicated dosages, followed by treatment with TB-peptide, and echocardiography was used to assess heart performance.

Consistent with literature and as expected, we observed that older mice were more susceptible to the toxic effects induced by lipopolysaccharide. The 24-month-old (aged) mice showed impaired cardiac function but were able to survive when receiving lipopolysaccharide challenged at 1 mg/kg. However, greater fatality was observed when lipopolysaccharide dose was increased to 3 mg/kg. In 10-week-old (young adult) mice, 3 mg/kg lipopolysaccharide triggered heart dysfunction without impact on survival, whereases at 10 mg/kg, we observed significant lipopolysaccharide-induced fatality in the group. Because of the different sensitivities to lipopolysaccharide between the aged and young adult mice, we were not able to choose a universal dose of lipopolysaccharide to induce cardiac dysfunction and to perform follow-up analysis in both groups. Therefore, we used the physiological function of the heart as a base for comparison in the studies performed in this report.

As shown in Figure 1A and 1B, at the levels of lipopolysaccharide challenge that inducing significant reduction in cardiac contractility in young or aged mice, administration of TB-peptide was able to rescue cardiac performance, demonstrated by its improvement in fractional shortening and ejection fraction. Further,

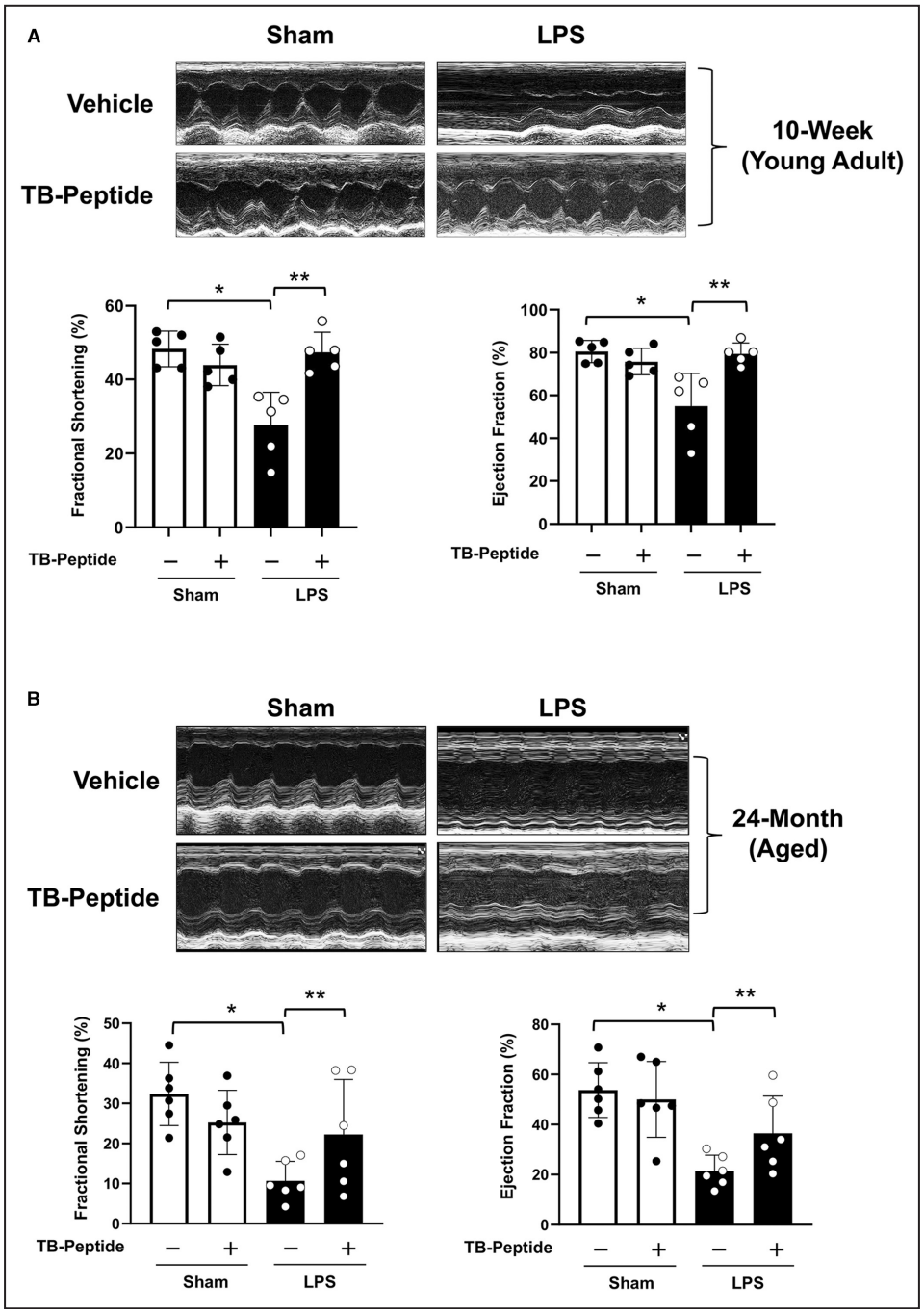

Figure 1. Cardiac protective effects of TB-peptide in young adult and aged mice during endotoxemia.

Mice were given 5 mg kg/lipopolysaccharide intraperitoneally and TB-peptide, 16 mg/kg, was administered intraperitoneally 30 minutes post lipopolysaccharide challenge. Experiments were performed 18 hours post challenge. Cardiac function was evaluated by echocardiography in the young adult (**A**, 5/group) and aged (**B**, 6/group) mice. Circulating cytokine levels were measured in blood serum prepared from the young adult (**C**, 5/group) and aged (**D**, 5/group) groups by ELISA. In harvested heart tissue, autophagy marker LC3II was detected by Western blot using the total tissue lysates, and signals were quantified by densitometry (**E**, 5/group). Levels of lactate were quantified in the heart tissue lysates (**F**, 5/group). All data were expressed as mean±SEM of at least 3 independent experiments. Data were analyzed by 2-way ANOVA with post hoc test for comparisons of multiple groups and Student *t* test for comparisons between 2 groups using GraphPad Prism software. Differences were considered statistically significant as $P \leq 0.05$. Significant differences are shown as * for sham vs lipopolysaccharide and ** for with vs without the treatment of TB-peptide (**A** through **E**) or for difference between age groups (**F**). IFN indicates interferon; IL, interleukin; LPS, lipopolysaccharide; and TNFα, tumor necrosis factor alpha.

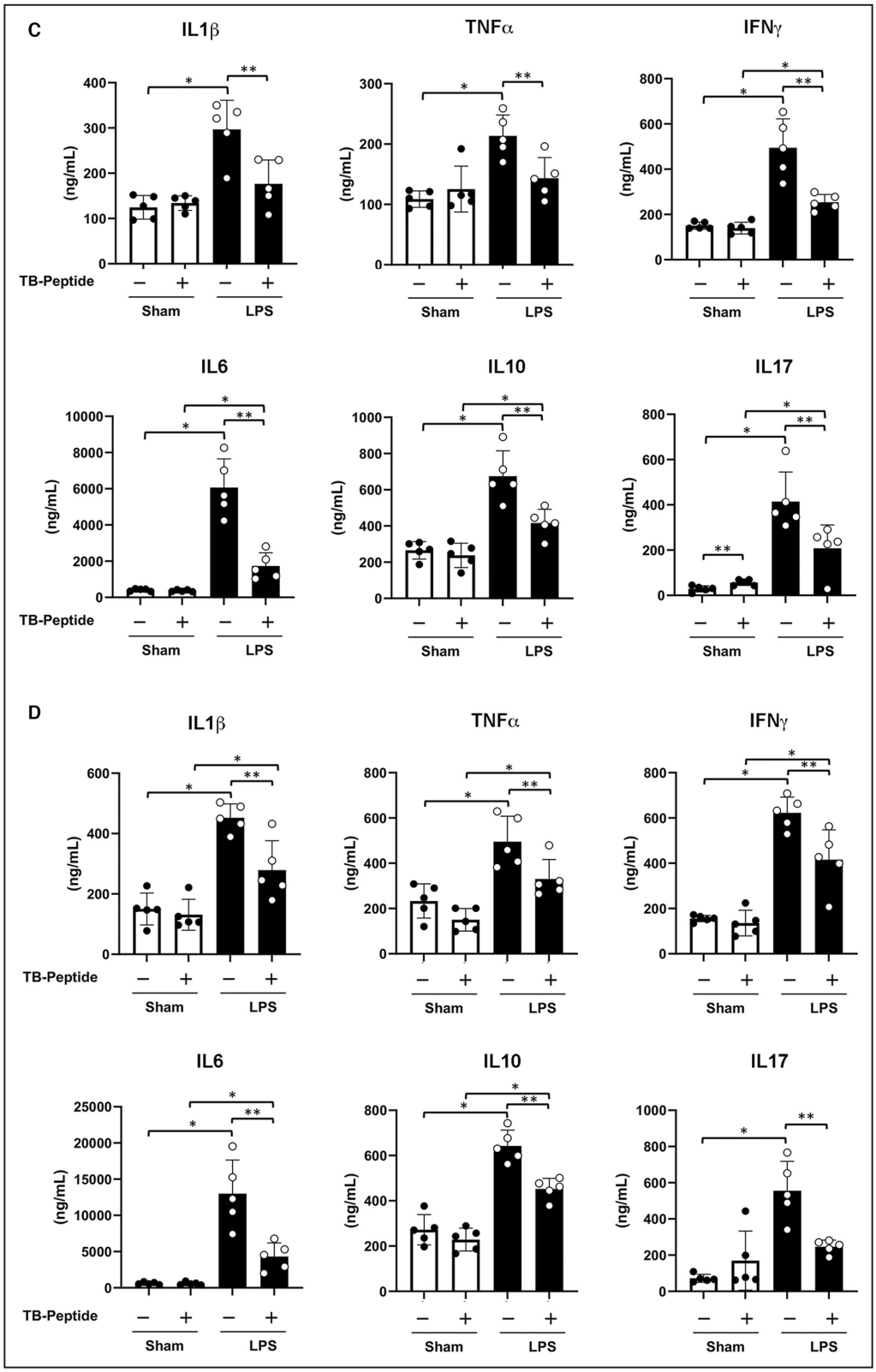

Figure 1. **Continued**

TB-peptide-mediated reduction in inflammation was demonstrated by its attenuation of circulating cytokines (Figure 1C and 1D). Consistent with published results in the literature from us and others,[18,21,33,34] we confirmed that this TB-peptide was able to boost cardiac autophagy response in both young and old animals during

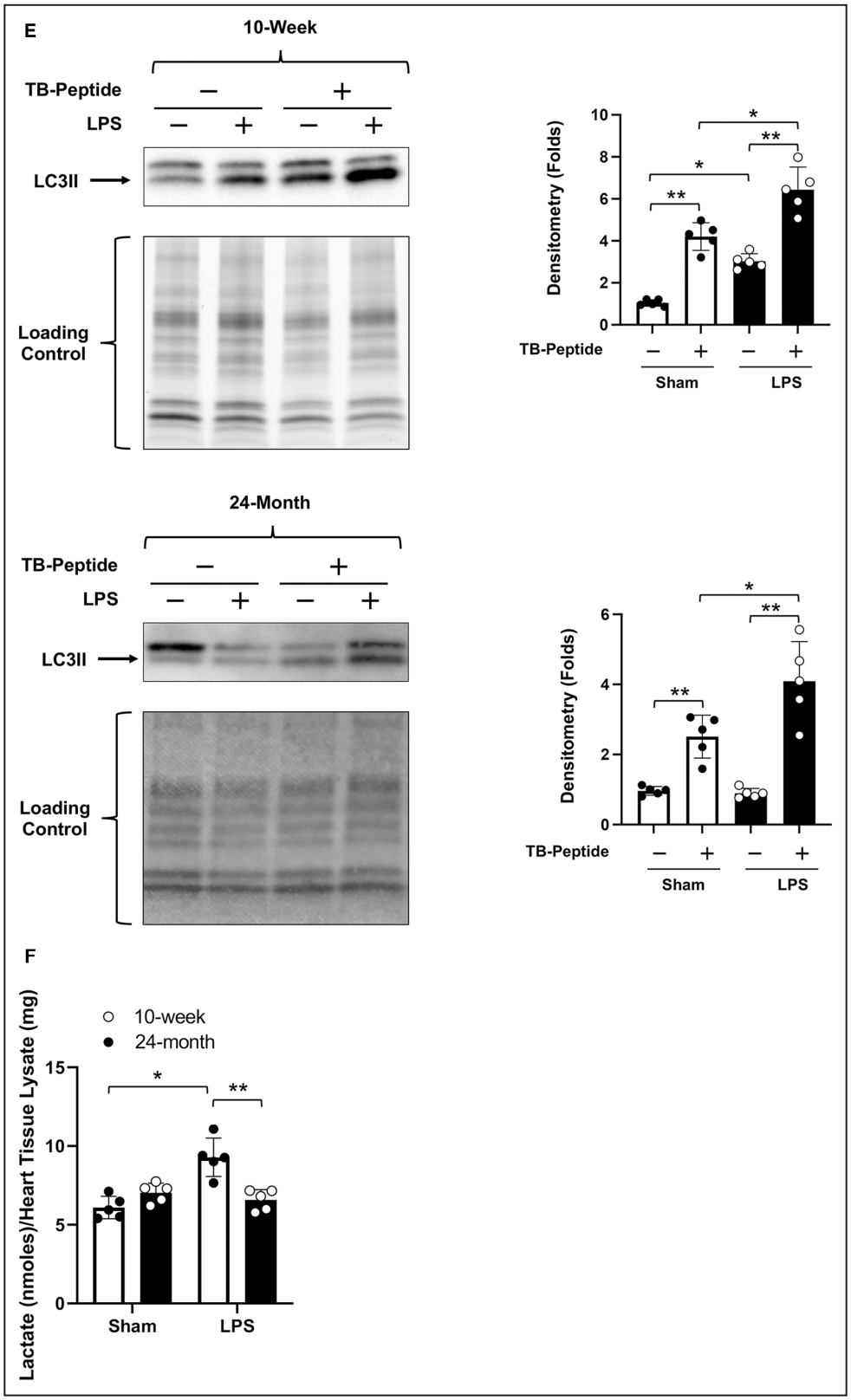

Figure 1. Continued

endotoxemia, shown by enhanced signal of LC3II in the heart tissue lysates (Figure 1E). Because lactate is a metabolic intermediate mediates both glucose metabolism and fatty acid metabolism, we measured levels of lactate in the heart tissue of 10-week-old and 24-month-old mice for the purpose of testing whether

cardiac performance associates with myocardial metabolic changes. We observed that lipopolysaccharide challenge produced a significant increase in lactate in young mice but not in old mice (Figure 1F), suggesting that lipopolysaccharide-stimulated shifting of cardiac energy metabolism is at least partially affected by aging.

A Targeted Metabolomics Study to Compare Myocardial Metabolite Profiling in Response to Endotoxemia and to the Follow-Up Therapeutic Treatment by TB-Peptide Between Young Adult and Aged Mice

LC–MS metabolomics analysis was applied to the heart tissue samples harvested from the experimental groups of young and aged mice subjected to lipopolysaccharide challenge or sham followed by treatment with TB-peptide or vehicle (Table 1).

A targeted approach was chosen, in which profiling covers 361 known metabolites that were selected based on published results showing their association with over 50 regulatory pathways in almost all aspects of myocardial metabolisms, such as central carbon metabolism (glycolysis tricarboxylic acid cycle, pentose phosphate), AA metabolism (branched-chain AAs, urea cycle), lipid metabolism (choline, fatty acids), and purine metabolism. Evaluation of data quality, exploratory analysis, and data preprocessing are summarized in Data S1. Across a total of 43 mouse heart samples, 156 metabolites were measured with detectable abundance, having missingness <20% and coefficient of variance <20% by univariate analysis. In the comparisons between groups, changes in metabolites showing false discovery rate of 10% or less were considered having statistical significance. As summarized in Table 2, lipopolysaccharide induced similar levels of significant changes in the number of metabolites in young and aged groups, 69 versus 62 respectively. In groups receiving TB-peptide, lipopolysaccharide altered levels of 42 metabolites in the young mice versus 60 in the aged mice. When under endotoxemia, TB-peptide altered 30 metabolites in the young versus 11 in the old mice. As expected, the peptide changed little or none in the sham controls of both young and aged groups. Analysis and comparisons of changes in metabolite profiles induced by endotoxemia and by TB-peptide in young and old mice are described in detail in the following sections.

Table 1. List of Animal Numbers Tested in Each Group

Age	Endotoxemia	Treatment	Number
Aged 24-mo	Sham	None	5
	Lipopolysaccharide		5
	Sham	TB-peptide	4
	Lipopolysaccharide		5
Young 10-wk	Sham	None	6
	Lipopolysaccharide		6
	Sham	TB-peptide	6
	Lipopolysaccharide		6

Myocardial Metabolite Profiling in Response to Endotoxemia and to the Follow-Up Therapeutic Treatment With TB-Peptide in Young Adult Mice

We first compared the metabolic profiles in the heart of young adult mice (10 weeks old) challenged with lipopolysaccharide or sham and their responses to the treatment with TB-peptide. Figure 2A summarized the interactive mean-difference plots of 4 comparison groups, including lipopolysaccharide-treated versus sham, lipopolysaccharide-challenged versus sham under the treatment of TB-peptide, sham group with peptide treatment versus untreated, and lipopolysaccharide group with peptide treatment versus untreated. Names of these metabolites, together with their values of log2-fold change (FC), average log2-abundance, and false discovery rate, are listed in Tables 3 through 5. Among the 156 targets with detectable significance, lipopolysaccharide challenge caused increases in 50 and decreases in 19 metabolites (Table 3). N-acetylglycine, a derivative of AA glycine metabolism, was shown the most increased metabolite with a 5.6-fold increase in response to lipopolysaccharide. Adenosine, whose derivatives function as energy carriers in forms of AMP, ADP, and ATP, was identified as the most significantly decreased metabolite with a change of over

Table 2. List of Numbers of Metabolites With Statistically Significant Changes

Experimental groups	Comparisons	Metabolites with changes in significance (false discovery rate <0.1)
Young 10-wk	Lipopolysaccharide vs sham	69
	Lipopolysaccharide vs sham under TB-peptide	42
	With vs without TB-peptide in shams	0
	With vs without TB-peptide in lipopolysaccharide challenged	30
Aged 24-mo	Lipopolysaccharide vs sham	62
	Lipopolysaccharide vs sham under TB-peptide	60
	With vs without TB-peptide in shams	1
	With vs without TB-peptide in lipopolysaccharide challenged	11

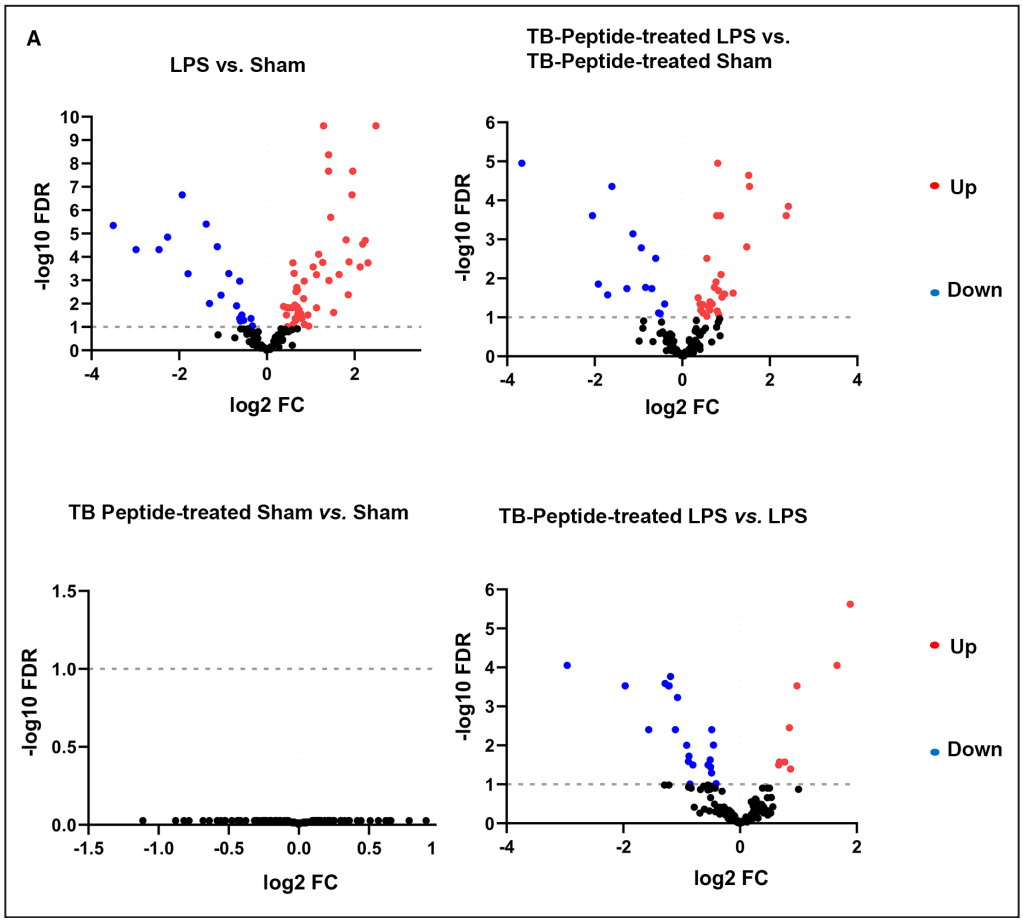

Figure 2. Analysis of lipopolysaccharide-induced changes in myocardial metabolites and the effects of TB-peptide in young mice.

Mice were given 5 mg/kg lipopolysaccharide intraperitoneally and heart tissues were harvested 18 hours later. **A**, Volcano plots generated using GraphPad Prism software showing metabolite-wise fold changes (log2 FC) plotted against false discovery rate (FDR, –log10 FDR). Significantly differentially abundant metabolites were indicated in red for upregulation and blue for downregulation (FDR ≤10%, FDR was determined using Benjamin-Hochberg procedure). **B**, Comparison of lipopolysaccharide-induced changes between groups with and without the treatment of TB-peptide. Degrees of fold change in abundance were shown in bar graphs. Results obtained from sham and lipopolysaccharide-challenged groups without the treatment of TB-peptide were shown in blue, and those from groups given treatment were shown in red. **C**, Metabolic pathways altered by lipopolysaccharide in the young hearts. **D**, TB-peptide-mediated regulation of metabolic pathways in the young hearts challenged by lipopolysaccharide. In (**C** and **D**) pathway analysis was performed by using Shiny GAM (integrated analysis of genes and metabolites) and Cytoscape software. Signaling networks were built on pathway clustering against the small molecule pathway database using MBRole 2.0 software. FC, fold change; FDR, false discovery rate; LPS, lipopolysaccharide; NAD, nicotinamide adenine dinucleotide; and UDP, Uridine diphosphate.

11-fold by lipopolysaccharide. As listed in Table 4, treatment with TB-peptide reduced the scope of lipopolysaccharide-induced changes in metabolites, which included upregulation in 28 and downregulation in 14 metabolites. The treatment also decreased the levels of changes. For example, lipopolysaccharide-triggered fold changes in N-acetyl-glycine and adenosine were reduced to 2.86 and 4.14 respectively, compared with 5.6 and 11 when TB-peptide was not given. However, in the case of UDP-glucose, an intermediate of synthesis of glycogen, lipopolysaccharides, and glycosphingolipids, the fold change of downregulation was increased from 7.9 to 12.67. As expected, TB-peptide did not incite detectable changes in sham animals, whereas the treatment increased the abundance in 8 but reduced in 22 metabolites in lipopolysaccharide-challenged groups (Table 5).

To further investigate the impact of TB-peptide in myocardial metabolites during endotoxemia, we compared the TB-peptide treated groups of sham and lipopolysaccharide-challenged mice with those without the treatment. As shown in Figure 2B, 31 metabolites

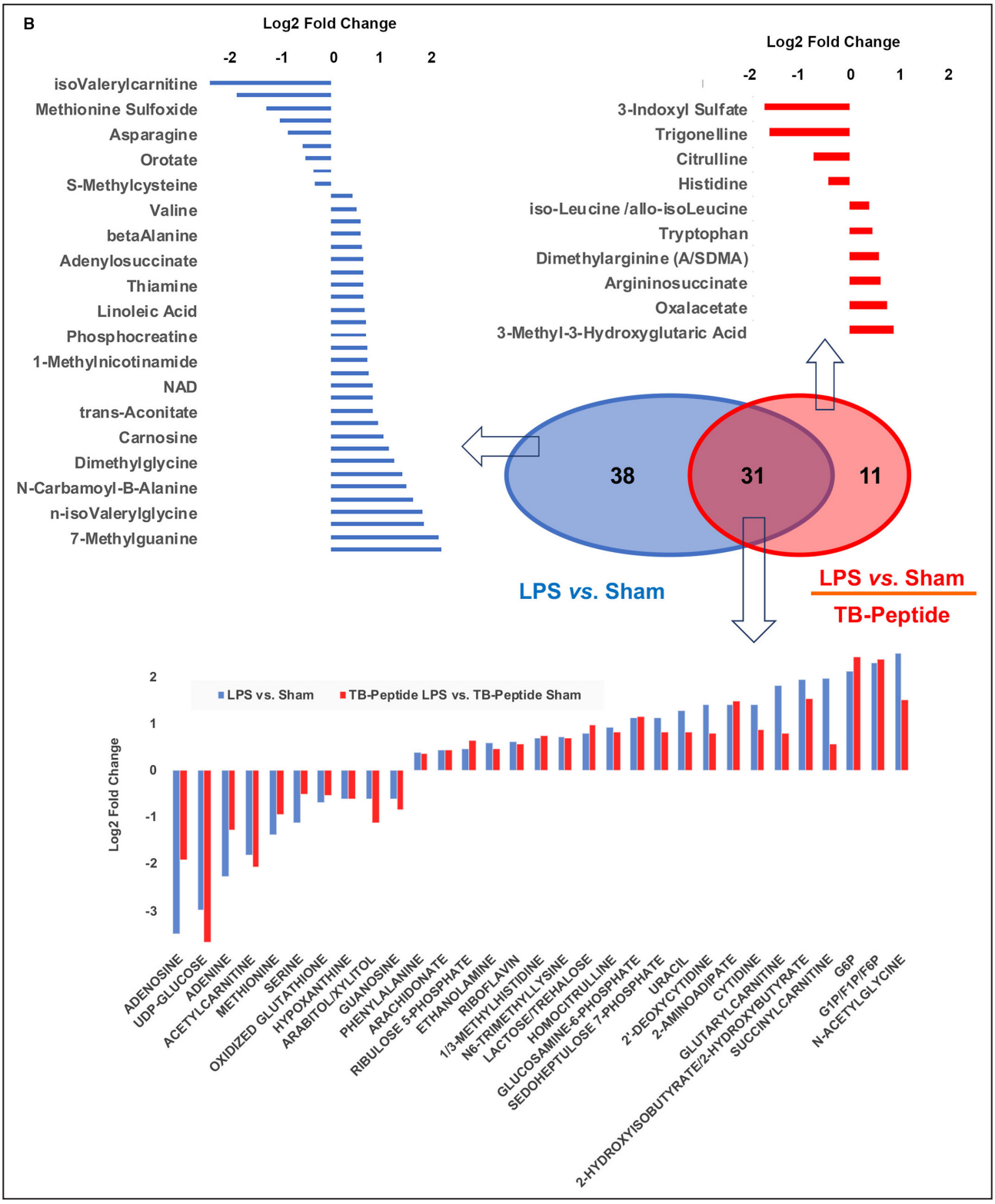

Figure 2. **Continued**

were identified as having lipopolysaccharide-associated changes regardless of the presence of TB-peptide. However, in more than half of these metabolites, lipopolysaccharide-associated fold changes were attenuated by TB-peptide, for example, in adenosine and N-acetyl-glycine. Additionally, lipopolysaccharide altered the abundance in 38 metabolites, which were not affected by TB-peptide. On the other hand, when

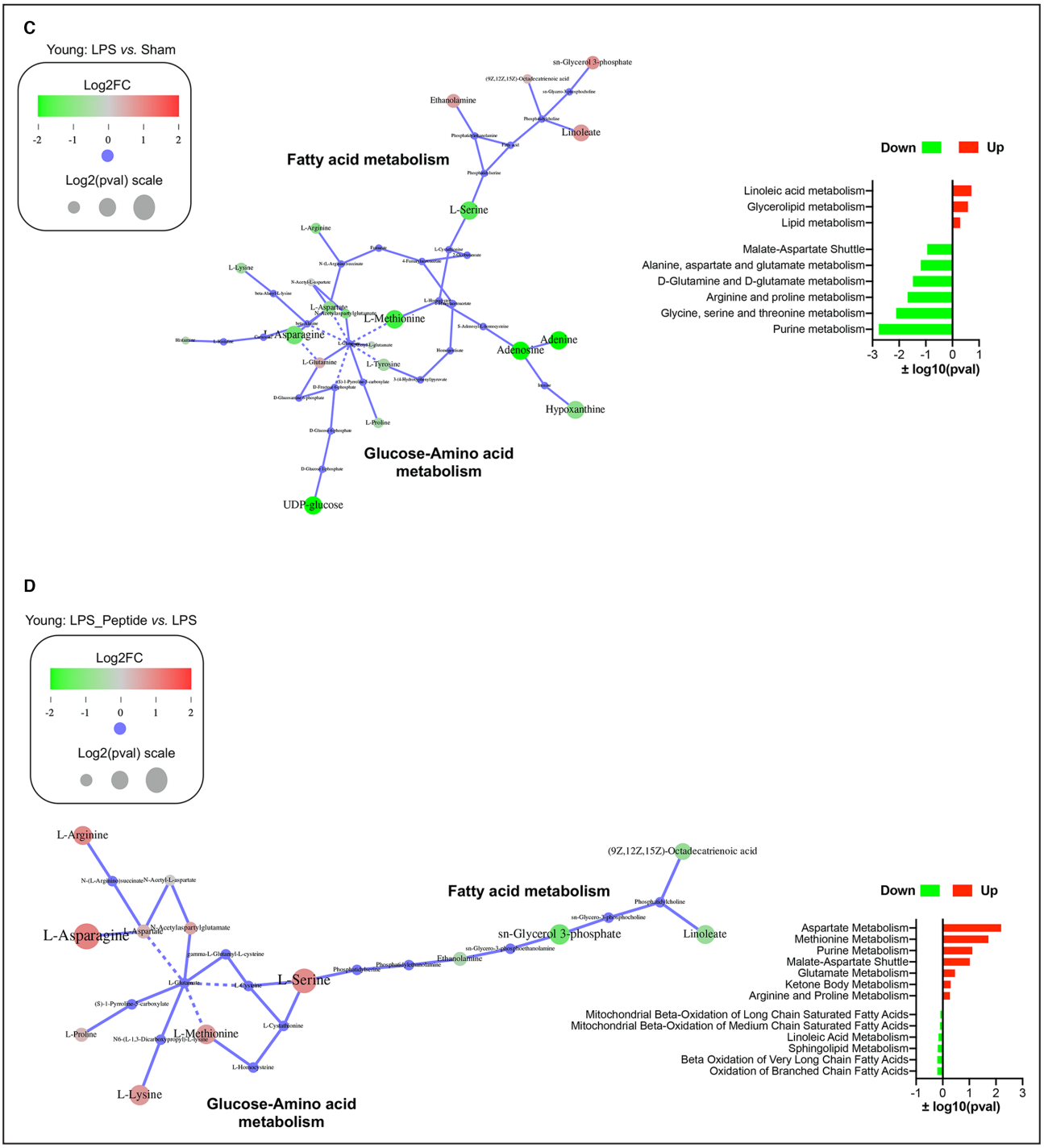

Figure 2. Continued

receiving TB-peptide treatment, lipopolysaccharide stimulated changes in 11 metabolites, which differences were not detectable in the absence of the peptide.

Using the data of metabolic changes summarized above, we performed pathway analysis using Shiny GAM and Cytoscape software and signaling network analysis based on the small molecule pathway database. Results showed that lipopolysaccharide significantly impaired pathways of carbohydrate/glucose metabolism and AA metabolism, including the malate–aspartate shuttle, D-glutamine/D-glutamate transition, alanine-aspartate–glutamate cycling, arginine-proline synthesis, glycine-serine–threonine pathway, and purine metabolism. In the meantime, lipopolysaccharide upregulated fatty acid metabolism, such as glycolipids and linoleic acid (Figure 2C). With the treatment of TB-peptide, the metabolism via AAs and glucose pathways was significantly improved whereas elevation in

Table 3. Lipopolysaccharide-Induced Significant Changes in Myocardial Metabolites of Young Mice

Metabolite	HMDB.ID	KEGG.ID	logFC	log2 abundance	FDR
Adenosine	HMDB00050	C00212	−3.504068696	23.86931938	4.5444E-06
UDP-glucose	HMDB00286	C00029	−2.982524074	17.63404042	4.86363E-05
isoValerylcarnitine	HMDB00688	C20826	−2.461951465	18.62973571	4.86363E-05
Adenine	HMDB00034	C00147	−2.266070291	21.22184279	1.42746E-05
Glycerophosphocholine	HMDB00086	C00670	−1.931798719	23.04142803	2.19963E-07
Acetylcarnitine	HMDB00201	C02571	−1.796429239	25.2547884	0.000521683
Methionine	HMDB00696	C00073	−1.383847973	18.29150982	3.94636E-06
Methionine sulfoxide	HMDB02005	C02989	−1.310180543	15.29682122	0.009896058
Serine	HMDB00187	C00065	−1.131081377	21.03427896	3.63156E-05
Pentothenate	HMDB00210	C00864	−1.047458243	22.34537951	0.004356857
Asparagine	HMDB00168	C00152	−0.868907953	19.14028377	0.000516636
Oxidized glutathione	HMDB03337	C00127	−0.69128763	21.8909802	0.012351006
Hypoxanthine	HMDB00157	C00262	−0.619501418	25.19445868	0.001094867
Arabitol/xylitol	HMDB00568	C01904	−0.617957822	17.20065105	0.043744604
Guanosine	HMDB00133	C00387	−0.603427381	19.31073305	0.055782705
Aspartic acid	HMDB00191	C00049	−0.570205387	22.25836953	0.030608556
Orotate	HMDB00226	C00295	−0.530918541	15.40333777	0.051914615
Tyrosine	HMDB00158	C00082	−0.363502257	20.3445506	0.043744604
S-methylcysteine	HMDB02108	C22040	−0.330426467	17.61812235	0.089455152
Phenylalanine	HMDB00159	C00079	0.381454602	22.22348415	0.013315853
o-phosphoethanolamine	HMDB0000224	C00346	0.44316751	22.59729909	0.014623415
Arachidonate	HMDB60102	C00219	0.445023154	22.35094198	0.030608556
Ribulose 5-phosphate	HMDB00618	C00199	0.468473027	21.6725341	0.097304299
Valine	HMDB00883	C00183	0.502650827	19.00666397	0.015100883
Ethanolamine	HMDB00149	C00189	0.582188606	15.43518173	0.014869146
N-Ac-alanine	HMDB00766		0.592545382	17.85330671	0.00017851
betaAlanine	HMDB00056	C00099	0.601495672	15.55146758	0.077722222
Riboflavin	HMDB00244	C00255	0.618958003	17.07767715	0.000507951
Anserine	HMDB00194	C01262	0.636848719	18.904511	0.011468999
Adenylosuccinate	HMDB00536	C03794	0.645779855	17.71677581	0.043744604
2-Hydroxyphenylacetate	HMDB62635	C01983	0.657154433	14.77089127	0.013315853
Thiamine	HMDB00235	C00378	0.661136726	19.02148908	0.050153061
N2, N2-dimethylguanosine	HMDB04824		0.664299123	13.74037868	0.003086691
Linoleic acid	HMDB00673	C01595	0.684098488	20.16085533	0.002001628
1/3-methylhistidine	HMDB00001	C01152	0.687300636	17.57160604	0.013624917
Uridine	HMDB00296	C00299	0.695257059	19.69582063	0.002563472
Phosphocreatine	HMDB01511	C02305	0.707007859	16.42740043	0.027285038
N6-trimethyllysine	HMDB01325	C03793	0.71827252	20.39412577	0.019355612
Cystathionine	HMDB00099	C02291	0.722192347	14.25041028	0.030608556
1-Methylnicotinamide	HMDB00699	C02918	0.732803892	17.65160318	0.018110501
Glycerol-3-P	HMDB00126	C00093	0.772364628	24.48432725	0.027019494
Lactose/trehalose	HMDB00186	C00243	0.795766699	18.98098587	0.043445742
NAD	HMDB00902	C00003	0.837197345	17.83782502	0.006131256
IMP	HMDB00175	C00130	0.8520967	26.20190769	0.001094867
trans-Aconitate	HMDB00958	C02341	0.854416958	13.41074106	0.076449306
Homocitrulline	HMDB00679	C02427	0.933493505	15.35924408	0.030608556
NADP	HMDB00217	C00006	0.952474872	12.74600768	0.092439731
Carnosine	HMDB00033	C00386	1.055365122	21.2161892	0.000267647

(*Continued*)

Table 3. Continued

Metabolite	HMDB.ID	KEGG.ID	logFC	log2 abundance	FDR
Glucosamine-6-phosphate	HMDB0001254	C00352	1.130319574	16.1179439	0.01520334
Sedoheptulose 7-phosphate	HMDB01068	C05382	1.132445025	21.99544532	0.000580224
3-Hydroxyisovaleric acid	HMDB00754	C20827	1.1786381	16.50883966	7.6863E-05
Dimethylglycine	HMDB00092	C01026	1.273851044	16.24965502	0.000174352
Uracil	HMDB00300	C00106	1.290287028	20.86123826	2.42562E-10
Cytidine	HMDB00089	C00475	1.406732689	21.73604314	2.14748E-08
2'-Deoxycytidine	HMDB00014	C00881	1.407228732	17.49697137	4.2482E-09
2-Aminoadipate	HMDB00510	C00956	1.41470616	16.87943741	0.001028555
1-Methyladenosine	HMDB03331	C02494	1.454698084	16.60747522	1.99942E-06
N-carbamoyl-B-alanine	HMDB00026	C02642	1.520205652	14.57996584	0.024131976
Allantoin	HMDB00462	C01551	1.647463659	20.63393545	0.000563337
Glutarylcarnitine	HMDB13130		1.807288491	17.65586613	1.85173E-05
n-isoValerylglycine	HMDB00678		1.854144069	15.97962302	0.00420179
3HBA	HMDB0000357	C01089	1.871241098	21.08722141	0.000162793
2-Hydroxyisobutyrate/2-hydroxybutyrate	HMDB00729		1.941624661	18.70370022	2.19963E-07
Succinylcarnitine	HMDB61717		1.957087967	23.05998206	2.14748E-08
G6P	HMDB0001401	C00092	2.126939231	26.42552439	0.000268097
7-Methylguanine	HMDB00897	C02242	2.184038818	15.09317898	2.82464E-05
Pseudouridine	HMDB00767	C02067	2.241822376	19.02450924	1.9771E-05
G1P/F1P/F6P	HMDB01586 HMDB01076 HMDB00124	C01094 C00085 C00103	2.305984672	24.44804743	0.00017851
N-AcetylGlycine	HMDB00532		2.48696726	16.97801982	2.42562E-10

3HBA, 3-hydroxybutyric acid; FC indicates fold change; FDR, false discovery rate; G6P, glucose 6-phosphate; IMP, inosine monophosphate; NAD, nicotinamide adenine dinucleotide; NADP, nicotinamide adenine dinucleotide phosphate; and UDP, uridine diphosphate.

fatty acid synthesis was attenuated (Figure 2D). These data suggest that the application of TB-peptide was able to rectify the alteration induced by lipopolysaccharide in heart of young adult mice, and thus, ameliorate cardiac function.

Myocardial Metabolite Profiling in Response to Endotoxemia and to the Follow-Up Therapeutic Treatment With TB-Peptide in Aged Mice

Similarly, the metabolic profiles in the hearts of aged mice (24 months old) from sham versus lipopolysaccharide-challenge groups and their responses to TB-peptide treatment were examined. The interactive mean-difference plots of 4 comparisons, including lipopolysaccharide-challenged versus sham, lipopolysaccharide-challenged versus sham under TB-peptide treatment, sham group with peptide treatment versus untreated, and lipopolysaccharide group with peptide treatment versus untreated, were summarized in Figure 3A. Metabolites detected with statistical significance, together with their values of fold change, average log2-abundance, and false discovery rate, are listed in Tables 6 through 8. Of the 156 metabolites, 24 targets were significantly elevated and 38 decreased by challenge with lipopolysaccharide (Table 6). Among these molecules, allantoin, the main product of uric acid oxidation, was increased the most, with a fold change of about 4.8, by lipopolysaccharide. On the other hand, as in the young mice, adenosine was identified as the most downregulated metabolite by lipopolysaccharide with a fold change of 3.2 in the heart of aged mice. In animals receiving TB-peptide, lipopolysaccharide triggered significant increases in 18 and decreases in 42 metabolites in the heart (Table 7). Under this condition, N-carbamoyl-β-alanine, a urea derivative of β-alanine, was the most upregulated metabolite with a fold-difference of 3.8, compared with the unchallenged sham controls. Lipopolysaccharide stimulated allantoin, but the fold difference was reduced to 3.3 by TB-peptide from 4.8 in the absence of the peptide treatment. Methionine sulfoxide, the oxidized form of methionine and a marker of oxidative stress, was found to be downregulated the most with a change of 2.5-fold. Interestingly, lipopolysaccharide-associated decrease in adenosine decrease was undetectable under the treatment of TB-peptide, suggesting a TB-peptide-mediated effect of improving energy production.

Table 4. Lipopolysaccharide-Induced Significant Changes in Myocardial Metabolites of Young Mice Receiving TB-Peptide

Metabolite	HMDB.ID	KEGG.ID	logFC	log2 abundance	FDR
UDP-glucose	HMDB00286	C00029	−3.663516753	17.63404042	1.11579E-05
Acetylcarnitine	HMDB00201	C02571	−2.051778059	25.2547884	0.000247391
Adenosine	HMDB00050	C00212	−1.917670301	23.86931938	0.014122908
3-indoxyl sulfate	HMDB00682		−1.70357922	17.91025929	0.026552223
Trigonelline	HMDB00875	C01004	−1.60698519	17.87022517	4.36735E-05
Adenine	HMDB00034	C00147	−1.262324222	21.22184279	0.018246811
Arabitol/xylitol	HMDB00568	C01904	−1.128885258	17.20065105	0.000723388
Methionine	HMDB00696	C00073	−0.935467711	18.29150982	0.001648547
Guanosine	HMDB00133	C00387	−0.837615621	19.31073305	0.016986526
Citrulline	HMDB00904	C00327	−0.696056936	22.13035679	0.018246811
Hypoxanthine	HMDB00157	C00262	−0.604536334	25.19445868	0.003084473
Oxidized glutathione	HMDB03337	C00127	−0.538028531	21.8909802	0.077134029
Serine	HMDB00187	C00065	−0.50558362	21.03427896	0.08018539
Histidine	HMDB00177	C00135	−0.400626334	22.92866174	0.045506699
Phenylalanine	HMDB00159	C00079	0.360855597	22.22348415	0.031563198
iso-Leucine/allo-isoLeucine	HMDB00172/ HMDB00557	C00407/ C21096	0.407011027	18.72100738	0.045506699
Arachidonate	HMDB60102	C00219	0.425021712	22.35094198	0.065189598
Tryptophan	HMDB00929	C00078	0.470281029	19.19353397	0.046864333
Ethanolamine	HMDB00149	C00189	0.47193374	15.43518173	0.077121862
Riboflavin	HMDB00244	C00255	0.561212469	17.07767715	0.003084473
Succinylcarnitine	HMDB61717		0.561678179	23.05998206	0.094145529
Dimethylarginine (A/SDMA)	HMDB01539/ HMDB03334	C03626	0.598466485	18.23516339	0.053269395
Argininosuccinate	HMDB00052	C03406	0.629467478	17.15747824	0.064830017
Ribulose 5-phosphate	HMDB00618	C00199	0.632741879	21.6725341	0.039872264
N6-Trimethyllysine	HMDB01325	C03793	0.681343752	20.39412577	0.045506699
1/3-Methylhistidine	HMDB00001	C01152	0.733773991	17.57160604	0.016986526
Oxalacetate	HMDB00223	C00036	0.772924705	13.77153688	0.012311173
2'-Deoxycytidine	HMDB00014	C00881	0.789242017	17.49697137	0.000247391
Glutarylcarnitine	HMDB13130		0.798260565	17.65586613	0.068927058
Uracil	HMDB00300	C00106	0.81276773	20.86123826	1.11579E-05
Sedoheptulose 7-phosphate	HMDB01068	C05382	0.830566254	21.99544532	0.020701305
Homocitrulline	HMDB00679	C02427	0.831176457	15.35924408	0.085314121
Cytidine	HMDB00089	C00475	0.871603261	21.73604314	0.000247391
Xanthosine	HMDB00299	C01762	0.887764943	16.32577761	0.007986437
3-Methyl-3-hydroxyglutaric acid	HMDB0000355	C03761	0.91046067	12.6291266	0.030332094
Lactose/trehalose	HMDB00186	C00243	0.966557408	18.98098587	0.025291865
Glucosamine-6-phosphate	HMDB0001254	C00352	1.163692793	16.1179439	0.023982594
2-Aminoadipate	HMDB00510	C00956	1.47129853	16.87943741	0.001561702
N-AcetylGlycine	HMDB00532		1.516513784	16.97801982	2.27301E-05
2-Hydroxyisobutyrate/2-hydroxybutyrate	HMDB00729		1.533744624	18.70370022	4.36735E-05
G1P/F1P/F6P	HMDB01586 HMDB01076 HMDB00124	C01094 C00085 C00103	2.376040124	24.44804743	0.000247391
G6P	HMDB0001401	C00092	2.42346041	26.42552439	0.000141886

FC indicates fold change; FDR, false discovery rate; UDP, uridine diphosphate.

Table 5. TB-Peptide-Induced Significant Changes in Myocardial Metabolites of Young Mice

Metabolite	HMDB.ID	KEGG.ID	logFC	log2 abundance	FDR
Lipopolysaccharide-challenged group					
n-isoValerylglycine	HMDB00678		−2.960102541	15.97962302	8.8989E-05
7-Methylguanine	HMDB00897	C02242	−1.967084102	15.09317898	0.000298167
Pseudouridine	HMDB00767	C02067	−1.564571918	19.02450924	0.003936741
N-AcetylGlycine	HMDB00532		−1.285854526	16.97801982	0.000257584
1-Methylnicotinamide	HMDB00699	C02918	−1.226467546	17.65160318	0.000298167
Succinylcarnitine	HMDB61717		−1.214433733	23.05998206	0.000297102
1-Methyladenosine	HMDB03331	C02494	−1.192026095	16.60747522	0.000170922
Trigonelline	HMDB00875	C01004	−1.106743314	17.87022517	0.003936741
3-Hydroxyisovaleric acid	HMDB00754	C20827	−1.071695407	16.50883966	0.000594075
Phosphocreatine	HMDB01511	C02305	−0.916614511	16.42740043	0.009986574
Glycerol-3-P	HMDB00126	C00093	−0.884612231	24.48432725	0.025786544
Dimethylglycine	HMDB00092	C01026	−0.873442773	16.24965502	0.01893279
Suberic acid	HMDB00893	C08278	−0.856700702	15.9663203	0.097925558
betaAlanine	HMDB00056	C00099	−0.809115183	15.55146758	0.031939882
Uridine	HMDB00296	C00299	−0.548756032	19.69582063	0.031939882
N2, N2-Dimethylguanosine	HMDB04824		−0.538285701	13.74037868	0.031939882
2'-Deoxycytidine	HMDB00014	C00881	−0.511869569	17.49697137	0.02353051
Cytidine	HMDB00089	C00475	−0.504341571	21.73604314	0.036253811
Linoleic acid	HMDB00673	C01595	−0.486995048	20.16085533	0.050989851
N-Ac-alanine	HMDB00766		−0.485510673	17.85330671	0.003936741
Uracil	HMDB00300	C00106	−0.45409582	20.86123826	0.009879525
Palmitic acid	HMDB0000220	C00249	−0.411652477	16.77132958	0.096541724
Methionine	HMDB00696	C00073	0.660600291	18.29150982	0.031939882
Lysine	HMDB00182	C00047	0.67590058	22.74349835	0.02672983
Argininosuccinate	HMDB00052	C03406	0.764288611	17.15747824	0.02672983
Serine	HMDB00187	C00065	0.844245287	21.03427896	0.003529375
Arginine	HMDB00517	C00062	0.86584688	22.91032246	0.040308837
Asparagine	HMDB00168	C00152	0.976183481	19.14028377	0.000298167
Pentothenate	HMDB00210	C00864	1.661249652	22.34537951	8.8989E-05
Glycerophosphocholine	HMDB00086	C00670	1.888270369	23.04142803	2.39539E-06
Sham group					
None	N/A	N/A	N/A	N/A	N/A

FC indicates fold change; and FDR, false discovery rate.

There was little effect of TB-peptide on cardiac metabolites in sham control animals; the only molecule with significant change was guanidinoacetate, showing a decrease of 2.3-fold (Table 8). In animals challenged by lipopolysaccharide, TB-peptide treatment led to decreases in 10 and an increase in 1 metabolite in aged hearts (Table 8).

The effects of TB-peptide on myocardial metabolites in aged mice during endotoxemia were also analyzed by comparing data from the TB-peptide treated groups of sham and lipopolysaccharide-challenged mice with those from animals without the treatment. As summarized in Figure 3B, 37 metabolites were identified having lipopolysaccharide-associated changes regardless of the presence of TB-peptide. However, in 18 of these molecules, lipopolysaccharide-induced fold changes were attenuated by TB-peptide. In addition, 25 metabolites that were altered by lipopolysaccharide but had little response to TB-peptide. Further, in animals given TB-peptide treatment, lipopolysaccharide altered 23 new metabolites compared with the condition of without the peptide treatment.

Metabolic profiling from the aged mice was applied to pathway analysis and network analysis as described previously. Results suggest that metabolites in pathways of glucose and amino acid metabolism were significantly downregulated in aged heart by endotoxemia (Figure 3C). Treatment with TB-peptide reversed the responses of these pathways (Figure 3D), consistent with the observations obtained in the young hearts.

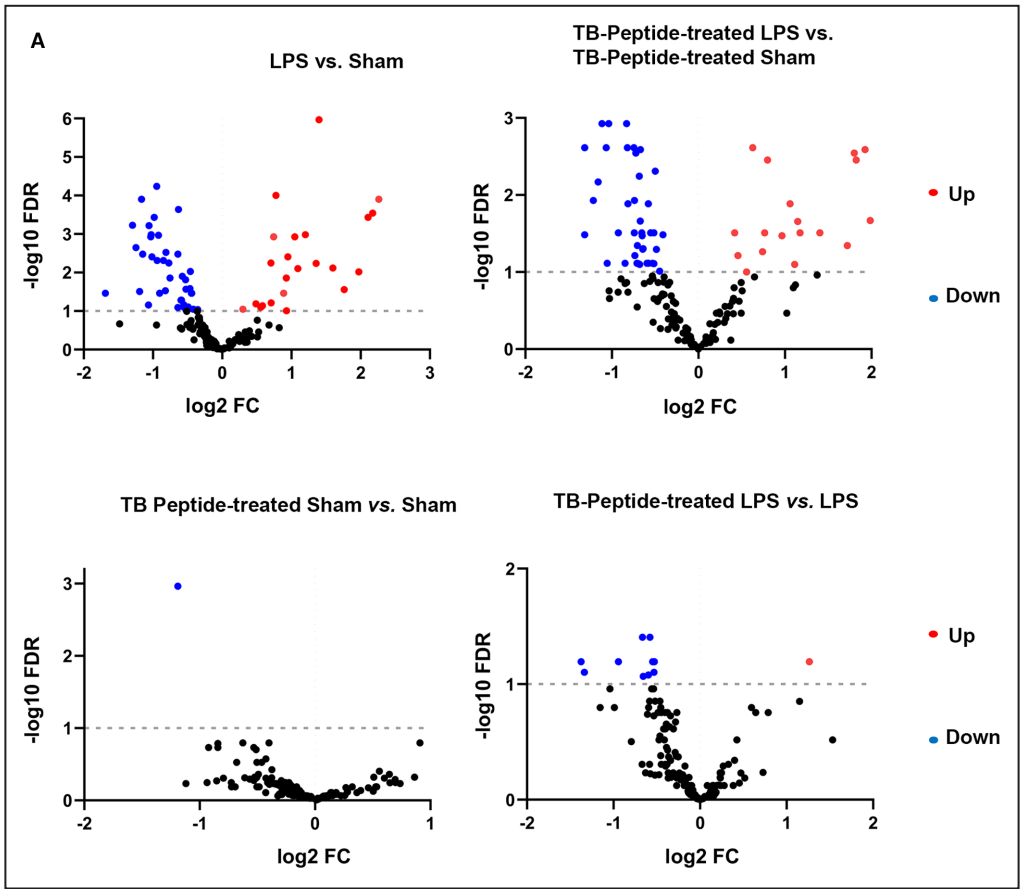

Figure 3. Analysis of lipopolysaccharide-induced changes in myocardial metabolites and the effects of TB-peptide in aged mice.

Mice were given 5 mg/kg lipopolysaccharide intraperitoneally and heart tissues were harvested 18 hours later. **A**, Volcano plots generated using GraphPad Prism software showing metabolite-wise fold changes (FC; log2 FC) plotted against false discovery rate (FDR; –log10 FDR). Significantly differentially abundant metabolites were indicated in red for upregulation and blue for downregulation (FDR ≤10%, FDR was determined using Benjamin-Hochberg procedure). **B**, Comparison of lipopolysaccharide-induced changes between groups with and without the treatment of TB-peptide. Degrees of fold change in abundance were shown in bar graphs. Results obtained from sham and lipopolysaccharide-challenged groups without the treatment of TB-peptide were shown in blue, and those from groups given treatment were shown in red. **C**, Metabolic pathways altered by lipopolysaccharide in the aged hearts. **D**, TB-peptide-mediated regulation of metabolic pathways in the aged hearts challenged by lipopolysaccharide. In (**C** and **D**) pathway analysis was performed by using Shiny GAM (integrated analysis of genes and metabolites) and Cytoscape software. Signaling networks were built on pathway clustering against the small molecule pathway database using MBRole 2.0 software. LPS indicates lipopolysaccharide.

However, unlike the young counterparts, lipopolysaccharide induced a decrease in fatty acid metabolism, and TB-peptide had little effect on this response.

Age-Dependent and -Independent Changes in Myocardial Metabolite Profiling in Response to Endotoxemia and to the Therapeutic Treatment by TB-Peptide

To address whether age plays an important role in altering myocardial metabolites in response to endotoxemia and to the treatment of TB-peptide, we compared compounds with significant changes between groups of young and old mice with or without lipopolysaccharide challenge and with or without the treatment of TB-peptide. As shown in Figure 4, the heatmap comparison indicates that TB-peptide mitigated lipopolysaccharide-induced impairment in amino acid biosynthesis via glutamate–aspartate pathway in both young and aged groups. A distinct age-dependent pattern was found to associate with metabolites involved in fatty acid metabolism, such as choline, phosphocholine, linolenic acid, linoleic acid, and 1-methylnicotinamide, as well as in AAs that were previously reported to be closely related to fatty acid

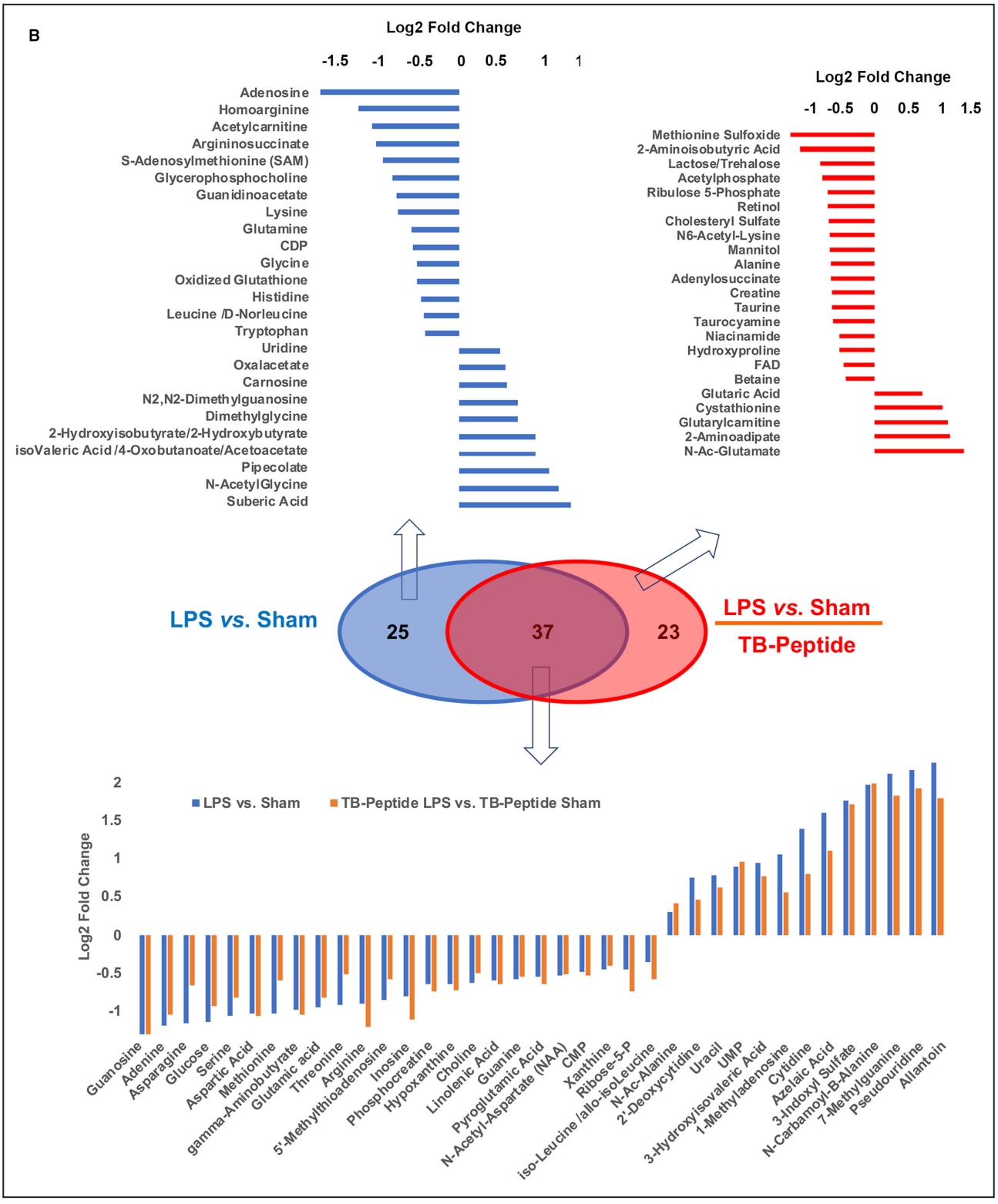

Figure 3. **Continued**

metabolism, such as isoleucine and valine.[35,36] In this category of molecules, TB-peptide appeared to attenuate lipopolysaccharide-induced changes in the young mice but had moderate or little effect in the aged group.

DISCUSSION

We previously demonstrated that promoting autophagy via Beclin-1 is cardiac protective in a mouse

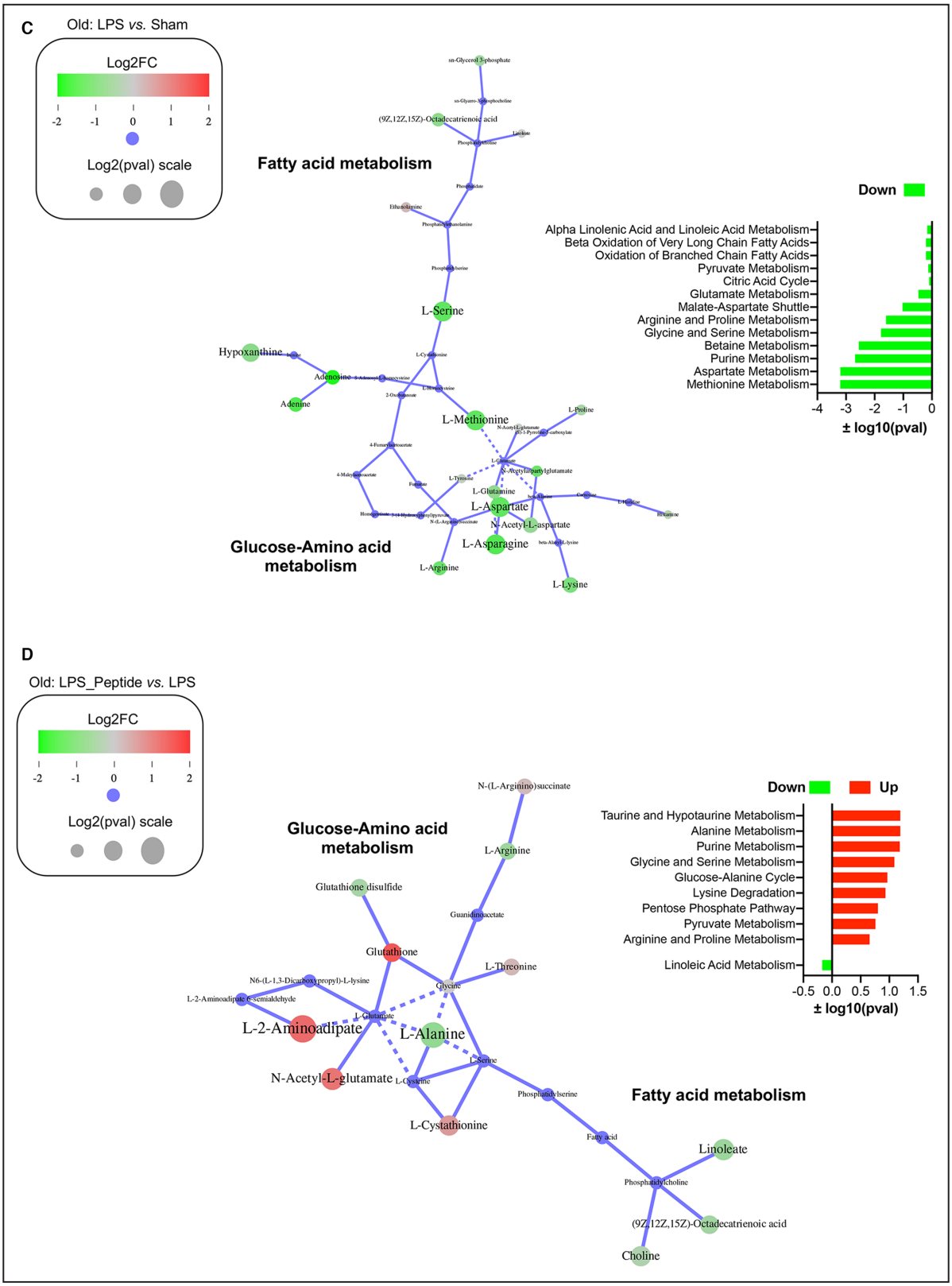

Figure 3. Continued

model of endotoxemia.[18] Additionally, pharmacological Beclin-1 activator TB-peptide exhibited therapeutic potential in several preclinical models including cancer chemotherapy,[25] infection,[32] endotoxemia,[18] and pneumonia-induced sepsis.[21] In the studies summarized here, we obtained results supporting that

Table 6. Lipopolysaccharide-Induced Significant Changes in Myocardial Metabolites of Old Mice

Metabolite	HMDB.ID	KEGG.ID	logFC	log2 abundance	FDR
Adenosine	HMDB00050	C00212	–1.688184448	23.86931938	0.034403039
Guanosine	HMDB00133	C00387	–1.29615317	19.31073305	0.000592696
Homoarginine	HMDB00670	C01924	–1.244909168	16.5631291	0.002257953
Adenine	HMDB00034	C00147	–1.193968535	21.22184279	0.030927489
Asparagine	HMDB00168	C00152	–1.163949669	19.14028377	0.000125369
Glucose	HMDB00122	C00031	–1.149712334	19.53764143	0.00333801
Acetylcarnitine	HMDB00201	C02571	–1.065199858	25.2547884	0.069306354
Serine	HMDB00187	C00065	–1.056593631	21.03427896	0.000609073
Methionine	HMDB00696	C00073	–1.031460638	18.29150982	0.001175991
Aspartic acid	HMDB00191	C00049	–1.026436549	22.25836953	0.001046276
Argininosuccinate	HMDB00052	C03406	–1.014001142	17.15747824	0.003901658
gamma-Aminobutyrate	HMDB0000112	C00334	–0.98214433	16.10830507	0.000368829
Glutamic acid	HMDB0000148	C00025	–0.947180143	25.43195443	5.79658E-05
S-adenosylmethionine (SAM)	HMDB01185	C00019	–0.941013935	19.99139517	0.004863305
Threonine	HMDB00167	C00188	–0.920342313	21.2053635	0.001079979
Arginine	HMDB00517	C00062	–0.903062039	22.91032246	0.034403039
5′-Methylthioadenosine	HMDB01173	C00170	–0.848063372	17.59340454	0.004863305
Glycerophosphocholine	HMDB00086	C00670	–0.820273511	23.04142803	0.029560383
Inosine	HMDB00195	C00294	–0.813289602	24.95825304	0.002993082
Guanidinoacetate	HMDB00128	C00581	–0.77012952	15.09248028	0.005676517
Lysine	HMDB00182	C00047	–0.75316112	22.74349835	0.013945565
Phosphocreatine	HMDB01511	C02305	–0.639635631	16.42740043	0.08049516
Hypoxanthine	HMDB00157	C00262	–0.638895878	25.19445868	0.00333801
Choline	HMDB00097	C00114	–0.630588455	24.40102471	0.000231462
Linolenic acid	HMDB01388	C06427	–0.596271721	15.63304987	0.051937091
Glutamine	HMDB00641	C00064	–0.586779963	26.15214756	0.051937091
Guanine	HMDB00132	C00242	–0.577276751	14.68578576	0.012447071
CDP	HMDB01546	C00112	–0.565056229	16.05522367	0.077007138
Pyroglutamic acid	HMDB00267	C01879	–0.553592863	17.61769228	0.069152505
N-acetyl-aspartate (NAA)	HMDB00812	C01042	–0.530288994	20.6742078	0.015436612
Glycine	HMDB00123	C00037	–0.52463187	16.90838982	0.027051637
Oxidized glutathione	HMDB03337	C00127	–0.524099062	21.8909802	0.092332756
CMP	HMDB00095	C00055	–0.492142473	16.81460482	0.078193582
Histidine	HMDB00177	C00135	–0.464033829	22.92866174	0.026268857
Xanthine	HMDB00292	C00385	–0.460122178	22.75835237	0.009396224
Ribose-5-P	HMDB01548	C00117	–0.444698791	23.26240744	0.034403039
Leucine /D-norleucine	HMDB00687	C00123	–0.441081153	21.86729067	0.034403039
Tryptophan	HMDB00929	C00078	–0.417622976	19.19353397	0.089792996
isoLeucine/alloisoLeucine	HMDB00172/ HMDB00557	C00407/ C21096	–0.354533541	18.72100738	0.091803245
N-Ac-alanine	HMDB00766		0.29875444	17.85330671	0.089792996
Uridine	HMDB00296	C00299	0.487820808	19.69582063	0.065195022
Oxalacetate	HMDB00223	C00036	0.557000664	13.77153688	0.079774023
Carnosine	HMDB00033	C00386	0.58247688	21.2161892	0.073075295
N2, N2-dimethylguanosine	HMDB04824		0.704513542	13.74037868	0.005676517
Dimethylglycine	HMDB00092	C01026	0.707705522	16.24965502	0.061281451
2'-Deoxycytidine	HMDB00014	C00881	0.744418915	17.49697137	0.001175991
Uracil	HMDB00300	C00106	0.777377648	20.86123826	9.99977E-05

(*Continued*)

Table 6. Continued

Metabolite	HMDB.ID	KEGG.ID	logFC	log2 abundance	FDR
UMP	HMDB0000288	C00105	0.888752926	20.76603231	0.034403039
2-Hydroxyisobutyrate/2-Hydroxybutyrate	HMDB00729		0.925103751	18.70370022	0.013945565
isoValeric acid/4-oxobutanoate/acetoacetate	HMDB00718/HMDB0001259	C08262/C00232/C00164	0.929126079	15.83124364	0.098653456
3-Hydroxyisovaleric acid	HMDB00754	C20827	0.947558894	16.50883966	0.003901658
1-Methyladenosine	HMDB03331	C02494	1.047461411	16.60747522	0.001175991
Pipecolate	HMDB00070	C00408	1.093309517	18.2965999	0.007891768
N-AcetylGlycine	HMDB00532		1.201641954	16.97801982	0.001046276
Suberic acid	HMDB00893	C08278	1.357470336	15.9663203	0.005774246
Cytidine	HMDB00089	C00475	1.39946568	21.73604314	1.08047E-06
Azelaic acid	HMDB00784	C08261	1.597627785	18.01963077	0.007585928
3-Indoxyl sulfate	HMDB00682		1.761797821	17.91025929	0.027607025
N-Carbamoyl-B-alanine	HMDB00026	C02642	1.973807696	14.57996584	0.009576727
7-Methylguanine	HMDB00897	C02242	2.106813609	15.09317898	0.000368829
Pseudouridine	HMDB00767	C02067	2.173259529	19.02450924	0.00028785
Allantoin	HMDB00462	C01551	2.263705109	20.63393545	0.000125369

FC indicates fold change; FDR, false discovery rate; and UMP, uridine 5'-monophosphate.

TB-peptide provides therapeutic benefits to alleviate sepsis-induced cardiomyopathy not only in young adults but also in aged population (Figure 1). Further, because autophagy intimately interacts with metabolic regulation,[37,38] we examined whether lipopolysaccharide challenge and the following TB-peptide treatment alter cardiac metabolism in young and aged mice by a targeted approach of metabolomic analysis. Our data revealed that a toxic challenge of lipopolysaccharide triggers both age-dependent and age-independent reprograming in energy metabolism in myocardium, and the effects of TB-peptide involve mitigating lipopolysaccharide-induced disturbance of carbohydrate and AA metabolism (Figures 2 through 4).

In sepsis, energy deficits, shown by abnormal accumulation of intermediates from breakdown of carbohydrates, lipids, and protein reserves, was found to associate with worsening outcomes, especially in nonsurvivors.[39,40] Sepsis responses such as high fever, the activation of immune cells, tachycardia, tachypnea, and the acute production of reactants demand a higher level of energy supplies. Evidence supports the hypothesis that, during the phase of early sepsis, a hypermetabolic response enables the body's defense mechanism to meet the needs of fighting against infection. However, late-stage sepsis is accompanied by hypometabolism leading to a severe disruption of metabolic homeostasis and creating a problem of metabolic deficiency. Prolonged hypometabolism is maladaptive because it generates a variety of toxic materials that stimulate inflammation and eventually provoke cell death and multiorgan dysfunction.[10,11]

Because autophagy is a self-survival mechanism via its "self-eating" capacity, promoting autophagy provides an opportunity to recycle the unwanted materials, such as damaged subcellular organelles, macro- and small molecules, that are used as replenished supplies for new biosynthesis.[41] Indeed, strategies that boost autophagy have been shown to have therapeutic promise in animal disease models including sepsis.[18,21,25,32] Testing potential therapeutic approaches in aged subjects is generally more challenging because of significantly reduced tolerance to stress conditions, likely a result of compromised immunity. Aged hearts are characterized as having decreased autophagy, accumulated mitochondrial damage, and higher venerability to acute insults such as sepsis.[42–44] Consistent with the hypothetical benefit of autophagy, overexpression of autophagy genes or long-term application of pharmacological autophagy inducers increased life span in various animal models.[33,45] In this present study, we obtained evidence showing that activation of autophagy by TB-peptide, when given post lipopolysaccharide-challenge, was able to improve cardiac performance and mitigate cytokine production in aged mice (Figure 1). The data suggest that a short-term application of autophagy inducer may effectively control sepsis-induced cardiomyopathy not only in young adults but also in an aged population.

One critical role of autophagy is to catalytically promote metabolic homeostasis under stress or disease conditions to meet the higher energy demand. In particular, autophagy is found to mediate the availability of carbohydrates, lipids, and nucleic acids through

Table 7. Lipopolysaccharide-Induced Significant Changes in Myocardial Metabolites of Old Mice Receiving TB-Peptide

Metabolite	HMDB.ID	KEGG.ID	logFC	log2 abundance	FDR
Methionine Sulfoxide	HMDB02005	C02989	−1.315359426	15.29682122	0.032800624
Guanosine	HMDB00133	C00387	−1.313846769	19.31073305	0.002429568
Arginine	HMDB00517	C00062	−1.213718583	22.91032246	0.011751792
2-Aminoisobutyric acid	HMDB01906	C03665	−1.15926623	16.87805146	0.006785659
Inosine	HMDB00195	C00294	−1.114049923	24.95825304	0.001187937
Aspartic acid	HMDB00191	C00049	−1.066506405	22.25836953	0.002429568
Adenine	HMDB00034	C00147	−1.054677043	21.22184279	0.077031359
gamma-Aminobutyrate	HMDB0000112	C00334	−1.036841123	16.10830507	0.001187937
Glucose	HMDB00122	C00031	−0.926049118	19.53764143	0.030927335
Lactose/trehalose	HMDB00186	C00243	−0.847024006	18.98098587	0.077031359
Glutamic acid	HMDB0000148	C00025	−0.82941974	25.43195443	0.001187937
Acetylphosphate	HMDB01494	C00227	−0.821693463	16.39466205	0.002429568
Serine	HMDB00187	C00065	−0.813524996	21.03427896	0.013011786
Ribose-5-P	HMDB01548	C00117	−0.745765832	23.26240744	0.002429568
Ribulose 5-phosphate	HMDB00618	C00199	−0.740587805	21.6725341	0.030927335
Retinol	HMDB00305	C19962	−0.73969727	15.36306034	0.011751792
Phosphocreatine	HMDB01511	C02305	−0.735301685	16.42740043	0.061264672
Hypoxanthine	HMDB00157	C00262	−0.723024619	25.19445868	0.002865168
Cholesteryl sulfate	HMDB00653	C18043	−0.71105748	19.13755507	0.077031359
N6-Acetyl-lysine	HMDB00206	C02727	−0.705562289	14.77645619	0.045328886
Mannitol	HMDB00765	C00392	−0.693679395	13.16532449	0.077782887
Alanine	HMDB00161	C00041	−0.682765355	22.92888413	0.005694127
Adenylosuccinate	HMDB00536	C03794	−0.679690864	17.71677581	0.079513095
Creatine	HMDB00064	C00300	−0.671114676	27.3962819	0.021813171
Taurine	HMDB00251	C00245	−0.669784967	25.54480293	0.002577699
Asparagine	HMDB00168	C00152	−0.654412013	19.14028377	0.030927335
Taurocyamine	HMDB03584	C01959	−0.649746984	18.41464737	0.033730157
Linolenic acid	HMDB01388	C06427	−0.642625434	15.63304987	0.050642956
Pyroglutamic acid	HMDB00267	C01879	−0.638746695	17.61769228	0.04959271
Methionine	HMDB00696	C00073	−0.593716604	18.29150982	0.077031359
isoLeucine/alloisoLeucine	HMDB00172 HMDB00557	C00407 C21096	−0.577791727	18.72100738	0.013011786
5′-Methylthioadenosine	HMDB01173	C00170	−0.577681568	17.59340454	0.077031359
Guanine	HMDB00132	C00242	−0.551389323	14.68578576	0.030927335
Niacinamide	HMDB01406	C00153	−0.548088152	24.36353105	0.030927335
Hydroxyproline	HMDB00725	C01157	−0.541960521	21.5717755	0.030927335
CMP	HMDB00095	C00055	−0.530365661	16.81460482	0.077031359
N-acetyl-aspartate (NAA)	HMDB00812	C01042	−0.515101634	20.6742078	0.030927335
Threonine	HMDB00167	C00188	−0.513380466	21.2053635	0.077782887
Choline	HMDB00097	C00114	−0.499772524	24.40102471	0.004912092
FAD	HMDB01248	C00016	−0.485262424	22.35700929	0.050903572
Betaine	HMDB00043	C00719	−0.447804269	26.20098847	0.097656148
Xanthine	HMDB00292	C00385	−0.410020205	22.75835237	0.032800624
N-Ac-alanine	HMDB00766		0.418995038	17.85330671	0.030927335
2′-Deoxycytidine	HMDB00014	C00881	0.456870328	17.49697137	0.061217759
1-Methyladenosine	HMDB03331	C02494	0.557048894	16.60747522	0.099733496
Uracil	HMDB00300	C00106	0.628604741	20.86123826	0.002429568
Glutaric acid	HMDB00661	C00489	0.740667826	14.45610428	0.054616457

(*Continued*)

Table 7. Continued

Metabolite	HMDB.ID	KEGG.ID	logFC	log2 abundance	FDR
3-Hydroxyisovaleric acid	HMDB00754	C20827	0.766584264	16.50883966	0.030927335
Cytidine	HMDB00089	C00475	0.799060305	21.73604314	0.00352042
UMP	HMDB0000288	C00105	0.965194771	20.76603231	0.033730157
Cystathionine	HMDB00099	C02291	1.059338163	14.25041028	0.013011786
Azelaic acid	HMDB00784	C08261	1.113138017	18.01963077	0.079513095
Glutarylcarnitine	HMDB13130		1.147225743	17.65586613	0.022110225
2-Aminoadipate	HMDB00510	C00956	1.175174657	16.87943741	0.030927335
N-Ac-glutamate	HMDB01138	C00624	1.403529606	14.71640701	0.030927335
3-Indoxyl sulfate	HMDB00682		1.721706893	17.91025929	0.045328886
Allantoin	HMDB00462	C01551	1.800469573	20.63393545	0.002865168
7-Methylguanine	HMDB00897	C02242	1.822720726	15.09317898	0.00352042
Pseudouridine	HMDB00767	C02067	1.924862053	19.02450924	0.002577699
N-carbamoyl-B-alanine	HMDB00026	C02642	1.984705127	14.57996584	0.021414052

FAD, flavin adenine dinucleotide; FC, fold change; FDR, false discovery rate; and UMP, uridine 5'-monophosphate.

selective signaling of glycophagy,[46,47] lipophagy,[48,49] DNAutophagy,[50] and RNAutophagy,[51] respectively. Therefore, reprograming cardiac metabolism is an expected response to the challenge of lipopolysaccharide, as well as to the treatment of TB-peptide. In this report, an established targeted metabolic approach was applied to examine major metabolic pathways of energy production using substrates of carbohydrates, AAs, and lipids. Our data suggest that endotoxemia shock caused an age-independent downregulation in glucose metabolism and AA metabolism, shown by changes in glucose, UDP-glucose, L-methionine, aspartate, and glutamate (Figures 2 and 3, Tables 3 and 6). This detected effect of endotoxemia on carbohydrate metabolism is consistent with previous report of lipopolysaccharide-induced impairment in myocardial glucose metabolism in an ex vivo perfused heart model.[6] We also found that TB-peptide exerted a reversing effect on these lipopolysaccharide-induced changes in metabolites, resulted in improved glucose and AAs metabolisms (Figures 2 and 3, Tables 4 and 7). It is worth pointing out that TB-peptide appears to have a stronger effect on AA metabolism, as summarized in the heatmap cluster analysis in Figure 4. In particular, TB-peptide protected metabolites generated via the glutamate–aspartate pathway from declines triggered by lipopolysaccharide.

Additionally, our data suggest that lipopolysaccharide challenge and the subsequent treatment of TB-peptide incite age-dependent responses of lipid metabolism in the heart. In the young group, lipopolysaccharide elevated levels of metabolites from lipid metabolism, such as glycolipids and linoleic acid (Figure 2 and Table 3). This observation is consistent

Table 8. TB-Peptide-Induced Significant Changes in Myocardial Metabolites of Old Mice

Metabolite	HMDB.ID	KEGG.ID	logFC	log2 abundance	FDR
Lipopolysaccharide-challenged group					
Cholecalciferol	HMDB00876	C05443	−1.374166031	14.2200854	0.063927243
Methionine sulfoxide	HMDB02005	C02989	−1.337112813	15.29682122	0.079081037
Cholesteryl sulfate	HMDB00653	C18043	−0.943755791	19.13755507	0.063927243
Acetylphosphate	HMDB01494	C00227	−0.666582046	16.39466205	0.039248283
cAMP	HMDB00058	C00575	−0.656493835	14.58770357	0.085577179
Creatine	HMDB00064	C00300	−0.597420557	27.3962819	0.083469536
Taurine	HMDB00251	C00245	−0.578446884	25.54480293	0.039248283
Alanine	HMDB00161	C00041	−0.547137941	22.92888413	0.063927243
Hydroxyproline	HMDB00725	C01157	−0.531313324	21.5717755	0.079081037
Ribose-5-P	HMDB01548	C00117	−0.526888538	23.26240744	0.063927243
2-Aminoadipate	HMDB00510	C00956	1.263245307	16.87943741	0.063927243
Sham group					
Guanidinoacetate	HMDB00128	C00581	−1.188381872	15.09248028	0.001083419

FC indicates fold change; and FDR, false discovery rate.

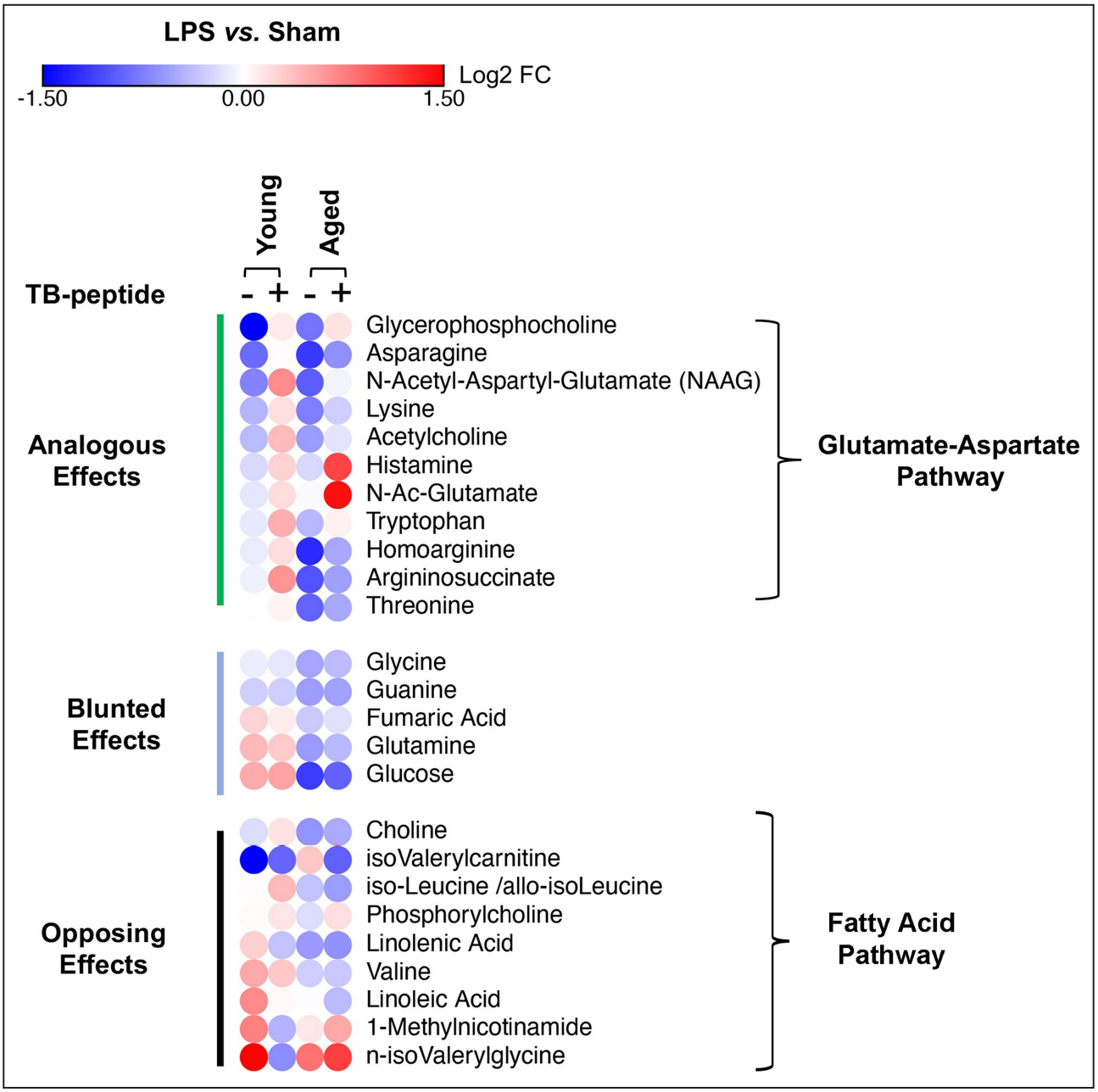

Figure 4. Comparison of lipopolysaccharide- and TB-peptide-associated changes in myocardial metabolites between young and aged mice.
Heatmaps and related clustering analysis of metabolites identified in the hearts of young and aged mice given lipopolysaccharide challenge or sham, with or without the treatment of TB-peptide, were compared. FC indicates fold change; and LPS, lipopolysaccharide.

with published results in literature.[52,53] For example, a clinic investigation detected a significant lipid accumulation in the myocardium of sepsis nonsurvivors.[52] Follow-up studies in animal models further suggest that this sepsis-associated phenomenon is likely caused by blocked fatty acid oxidation due to impaired regulation via transcription factor peroxisome proliferator-activated receptor-α.[53] In our study presented herein, we found that the lipopolysaccharide-induced increases in lipid metabolites were attenuated by the treatment with TB-peptide (Figure 2 and Table 4). A plausible mechanism of this peptide-mediated effect is that promoting autophagy improves the clearance of wasted molecules and thus reduces lipid accumulation. In addition, a boost in autophagy may improve the overall QC of the mitochondria pool in the heart and thus enhance the use of fatty acid substrates for production of energy. However, in the aged hearts, we observed that lipopolysaccharide mediated a moderate yet significant downregulation trend in fatty acids,

with little effect of TB-peptide (Figure 3 and Tables 6 through 8).

Whether the lipopolysaccharide-mediated decrease in lipids is pathological to the aged hearts remains to be further investigated. One point to consider is that myocardial lipid accumulation and impairment of fatty acid use increase with age.[54] Thus, because of a relatively higher baseline levels of lipids, lipid changes in the aged hearts may not be as dramatic as those in the young groups in response to external stimuli such as lipopolysaccharide. Similarly, postchallenge administration of TB-peptide to temporally induce autophagy is unlikely to affect lipid levels in the heart. Nonetheless, knowledge regarding the age-associated difference in fatty acid metabolism in septic hearts is still limited. Whether the expression and enzymatic activities of fatty acid metabolic factors alter with age, and whether these changes are reprogramed in response to septic challenge and autophagy stimulation, are critical to better understand the mechanism-of-action of TB-peptide. Furthermore, in sepsis, dysfunctional mitochondria and disrupted lipid metabolism were also observed in mitochondria-enriched organs other than the heart, such as in muscle and liver.[55] Measurements of levels of metabolic substrates of glucose, lactate, and pyruvate in a porcine model of endotoxemia suggest that myocardium and skeletal muscle share a similar pattern of changes.[56] Thus, increasing autophagy capacity by activating Beclin-1 via TB-peptide may have an effect to alleviate muscle atrophy and liver dysfunction. This potential effect and its possible association with aging require further evaluation.

CONCLUSIONS

Taken together, in this report, we provided evidence showing that Beclin-1 activating TB-peptide possesses therapeutic potential for sepsis-induced cardiomyopathy in both young and aged populations. A pilot metabolic study using a targeted metabolomics analysis has linked this beneficial effect to improvements in carbohydrate and AA metabolism. Future studies are warranted to determine the functional changes of regulatory signaling factors in these events. Furthermore, given the limited number of metabolites measured in targeted metabolomic profiles (albeit with high sensitivity), application of an untargeted metabolomics approach may reveal a broader range of cardiac metabolites impactaffecteded by age, lipopolysaccharide, and TB-peptide. It is also recognized that sepsis-induced changes in metabolic homeostasis progresses with severity and depends on the context of tissue and/or cell types. For example, in a mouse model of endotoxemia, lipopolysaccharide challenge decreases lipid levels in the blood while increasing then in the liver, suggesting a possibility of transporting lipids to the liver as a potential energy source.[57] Further, different types of shock conditions appear to stimulate distinct metabolic pathways; such difference was found in the heart and muscle when models of endotoxemia and hemorrhage shock were compared.[58] Lastly, though the endotoxemia model has been widely used as an experimental model mimicking the overwhelming inflammation state at the initial phase of human sepsis, studies in models of infection-induced sepsis, such as cecal ligation and punction sepsis or pneumonia sepsis, are expected to reveal more in-depth knowledge of relevance with clinical status and/or pathogen specificity. In a recent study, we obtained promising results suggesting that TB-peptide has a therapeutic potential in control of pulmonary pathology in a mouse model of pneumonia sepsis.[21] Future evaluation of metabolic reprograming at different sepsis models, stages of sepsis, and in different organs could help identify metabolic chemicals and/or regulatory enzymes as diagnostic markers and drug targets for sepsis. Eventually, studies in this area are expected to develop strategies for improving metabolic plasticity as potential new and effective therapies.

ARTICLE INFORMATION

Received January 7, 2022; accepted June 2, 2022.

Affiliations

Department of Surgery, Burn & Shock Trauma Research Institute, Loyola University Chicago Stritch School of Medicine, Maywood, IL (M.K., A.N., Q.S.Z.); Department of Biological Sciences, Rice University, Houston, TX (R.Z.); Department of Surgery, University of South Florida, Tampa, FL (D. Ren, Z.H., J.L.); Department of Environmental and Occupational Health Sciences (L.W.); and Department of Anesthesiology and Pain Medicine, Northwest Metabolomics Research Center (D.D., D. Raftery, H.P.), University of Washington, Seattle, WA; Department of Lab Medicine & Pathology (D.P.); and Department of Biology (D.P.), University of Washington School of Medicine, Seattle, WA; Department of Surgery (Y.S.); Department of Immunology (M.G.) and Cardiology Division, Department of Internal Medicine (Q.-J.Z., Z.-P.L.), University of Texas Southwestern Medical Center, Dallas, TX.

Sources of Funding

This work is supported by Nathan Shock Center Pilot Award (to Zang), National Institutes of Health (NIH) grant 2R01GM111295-01 (to Zang), HL109471 and CA215063 (to Liu), American Heart Association grant AHA 19TP34910172 (to Liu), NIH R01HL158515 and R01GM124108 (to Li), R01AG049494 (to Promislow), NIH P30 AG013280 (to the University of Washington Nathan Shock Center), and NIH S10 Grant 1S10OD021562-01 (to Raftery) which funded a purchase of the LC–MS system used to acquire targeted metabolomics data. The NIH Common Fund's National Metabolomics Data Repository website, the Metabolomics Workbench, is supported by NIH grant U2C-DK119886.

Disclosures

None.

Supplemental Material

Data S1

REFERENCES

1. Singer M, Deutschman CS, Seymour CW, Shankar-Hari M, Annane D, Bauer M, Bellomo R, Bernard GR, Chiche JD, Coopersmith CM, et al.

The third international consensus definitions for sepsis and septic shock (Sepsis-3). *JAMA*. 2016;315:801–810. doi: 10.1001/jama.2016.0287
2. Levy MM, Dellinger RP, Townsend SR, Linde-Zwirble WT, Marshall JC, Bion J, Schorr C, Artigas A, Ramsay G, Beale R, et al. The Surviving Sepsis Campaign: results of an international guideline-based performance improvement program targeting severe sepsis. *Crit Care Med*. 2010;38:367–374. doi: 10.1097/CCM.0b013e3181cb0cdc
3. Iwashyna TJ, Ely EW, Smith DM, Langa KM. Long-term cognitive impairment and functional disability among survivors of severe sepsis. *JAMA*. 2010;304:1787–1794. doi: 10.1001/jama.2010.1553
4. Zanotti-Cavazzoni SL, Hollenberg SM. Cardiac dysfunction in severe sepsis and septic shock. *Curr Opin Crit Care*. 2009;15:392–397. doi: 10.1097/MCC.0b013e3283307a4e
5. Drosatos K, Drosatos-Tampakaki Z, Khan R, Homma S, Schulze PC, Zannis VI, Goldberg IJ. Inhibition of c-Jun-N-terminal kinase increases cardiac peroxisome proliferator-activated receptor alpha expression and fatty acid oxidation and prevents lipopolysaccharide-induced heart dysfunction. *J Biol Chem*. 2011;286:36331–36339. doi: 10.1074/jbc.M111.272146
6. Tessier JP, Thurner B, Jungling E, Luckhoff A, Fischer Y. Impairment of glucose metabolism in hearts from rats treated with endotoxin. *Cardiovasc Res*. 2003;60:119–130. doi: 10.1016/S0008-6363(03)00320-1
7. Langley RJ, Tsalik EL, van Velkinburgh JC, Glickman SW, Rice BJ, Wang C, Chen B, Carin L, Suarez A, Mohney RP, et al. An integrated clinico-metabolomic model improves prediction of death in sepsis. *Sci Transl Med*. 2013;5:195ra95. doi: 10.1126/scitranslmed.3005893
8. Protti A, Carre J, Frost MT, Taylor V, Stidwill R, Rudiger A, Singer M. Succinate recovers mitochondrial oxygen consumption in septic rat skeletal muscle. *Crit Care Med*. 2007;35:2150–2155. doi: 10.1097/01.ccm.0000281448.00095.4d
9. Zang Q, Maass DL, Tsai SJ, Horton JW. Cardiac mitochondrial damage and inflammation responses in sepsis. *Surg Infect*. 2007;8:41–54. doi: 10.1089/sur.2006.033
10. Soares MP, Gozzelino R, Weis S. Tissue damage control in disease tolerance. *Trends Immunol*. 2014;35:483–494. doi: 10.1016/j.it.2014.08.001
11. Balmer ML, Hess C. Starving for survival-how catabolic metabolism fuels immune function. *Curr Opin Immunol*. 2017;46:8–13. doi: 10.1016/j.coi.2017.03.009
12. Van Wyngene L, Vandewalle J, Libert C. Reprogramming of basic metabolic pathways in microbial sepsis: therapeutic targets at last? *EMBO Mol Med*. 2018;10:e8712. doi: 10.15252/emmm.201708712
13. Gustafsson AB, Gottlieb RA. Heart mitochondria: gates of life and death. *Cardiovasc Res*. 2008;77:334–343. doi: 10.1093/cvr/cvm005
14. Zang QS, Sadek H, Maass DL, Martinez B, Ma L, Kilgore JA, Williams NS, Frantz DE, Wigginton JG, Nwariaku FE, et al. Specific inhibition of mitochondrial oxidative stress suppresses inflammation and improves cardiac function in a rat pneumonia-related sepsis model. *Am J Physiol Heart Circ Physiol*. 2012;302:H1847–H1859. doi: 10.1152/ajpheart.00203.2011
15. Zang QS, Maass DL, Wigginton JG, Barber RC, Martinez B, Idris AH, Horton JW, Nwariaku FE. Burn serum causes a CD14-dependent mitochondrial damage in primary cardiomyocytes. *Am J Physiol Heart Circ Physiol*. 2010;298:H1951–H1958. doi: 10.1152/ajpheart.00927.2009
16. Zang QS, Martinez B, Yao X, Maass DL, Ma L, Wolf SE, Minei JP. Sepsis-induced cardiac mitochondrial dysfunction involves altered mitochondrial-localization of tyrosine kinase Src and tyrosine phosphatase SHP2. *PLoS One*. 2012;7:e43424. doi: 10.1371/journal.pone.0043424
17. Mizushima N, Levine B. Autophagy in mammalian development and differentiation. *Nat Cell Biol*. 2010;12:823–830. doi: 10.1038/ncb0910-823
18. Sun Y, Yao X, Zhang QJ, Zhu M, Liu ZP, Ci B, Xie Y, Carlson D, Rothermel BA, Sun Y, et al. Beclin-1-dependent autophagy protects the heart during sepsis. *Circulation*. 2018;138:2247–2262. doi: 10.1161/CIRCULATIONAHA.117.032821
19. Liang XH, Kleeman LK, Jiang HH, Gordon G, Goldman JE, Berry G, Herman B, Levine B. Protection against fatal Sindbis virus encephalitis by beclin, a novel Bcl-2-interacting protein. *J Virol*. 1998;72:8586–8596. doi: 10.1128/JVI.72.11.8586-8596.1998
20. Liang XH, Jackson S, Seaman M, Brown K, Kempkes B, Hibshoosh H, Levine B. Induction of autophagy and inhibition of tumorigenesis by beclin 1. *Nature*. 1999;402:672–676. doi: 10.1038/45257
21. Nikouee A, Kim M, Ding X, Sun Y, Zang QS. Beclin-1-dependent autophagy improves outcomes of pneumonia-induced sepsis. *Front Cell Infect Microbiol*. 2021;11:706637. doi: 10.3389/fcimb.2021.706637
22. Sun Y, Cai Y, Qian S, Chiou H, Zang QS. Beclin-1 improves mitochondria-associated membranes in the heart during endotoxemia. *FASEB Bioadv*. 2021;3:123–135. doi: 10.1096/fba.2020-00039
23. Sud M, Fahy E, Cotter D, Azam K, Vadivelu I, Burant C, Edison A, Fiehn O, Higashi R, Nair KS, et al. Metabolomics Workbench: an international repository for metabolomics data and metadata, metabolite standards, protocols, tutorials and training, and analysis tools. *Nucleic Acids Res*. 2016;44:D463–D470. doi: 10.1093/nar/gkv1042
24. Kadioglu A, Cuppone AM, Trappetti C, List T, Spreafico A, Pozzi G, Andrew PW, Oggioni MR. Sex-based differences in susceptibility to respiratory and systemic pneumococcal disease in mice. *J Infect Dis*. 2011;204:1971–1979. doi: 10.1093/infdis/jir657
25. Pietrocola F, Pol J, Vacchelli E, Rao S, Enot DP, Baracco EE, Levesque S, Castoldi F, Jacquelot N, Yamazaki T, et al. Caloric restriction mimetics enhance anticancer immunosurveillance. *Cancer Cell*. 2016;30:147–160. doi: 10.1016/j.ccell.2016.05.016
26. Gao S, Ho D, Vatner DE, Vatner SF. Echocardiography in mice. *Curr Protoc Mouse Biol*. 2011;1:71–83. doi: 10.1002/9780470942390.mo100130
27. Li X, Liu J, Hu H, Lu S, Lu Q, Quan N, Rousselle T, Patel MS, Li J. Dichloroacetate ameliorates cardiac dysfunction caused by ischemic insults through AMPK signal pathway-not only shifts metabolism. *Toxicol Sci*. 2019;167:604–617. doi: 10.1093/toxsci/kfy272
28. Miklas JW, Clark E, Levy S, Detraux D, Leonard A, Beussman K, Showalter MR, Smith AT, Hofsteen P, Yang X, et al. TFPa/HADHA is required for fatty acid beta-oxidation and cardiolipin re-modeling in human cardiomyocytes. *Nat Commun*. 2019;10:4671. doi: 10.1038/s41467-019-12482-1
29. Wei R, Wang J, Su M, Jia E, Chen S, Chen T, Ni Y. Missing value imputation approach for mass spectrometry-based metabolomics data. *Sci Rep*. 2018;8:663. doi: 10.1038/s41598-017-19120-0
30. Ritchie ME, Phipson B, Wu D, Hu Y, Law CW, Shi W, Smyth GK. Limma powers differential expression analyses for RNA-sequencing and microarray studies. *Nucleic Acids Res*. 2015;43:e47. doi: 10.1093/nar/gkv007
31. Smyth GK. Linear models and empirical bayes methods for assessing differential expression in microarray experiments. *Stat Appl Genet Mol Biol*. 2004;3:Article3. doi: 10.2202/1544-6115.1027
32. Shoji-Kawata S, Sumpter R, Leveno M, Campbell GR, Zou Z, Kinch L, Wilkins AD, Sun Q, Pallauf K, MacDuff D, et al. Identification of a candidate therapeutic autophagy-inducing peptide. *Nature*. 2013;494:201–206. doi: 10.1038/nature11866
33. Fernandez AF, Sebti S, Wei Y, Zou Z, Shi M, McMillan KL, He C, Ting T, Liu Y, Chiang WC, et al. Disruption of the beclin 1-BCL2 autophagy regulatory complex promotes longevity in mice. *Nature*. 2018;558:136–140. doi: 10.1038/s41586-018-0162-7
34. Lee S, Lee SJ, Coronata AA, Fredenburgh LE, Chung SW, Perrella MA, Nakahira K, Ryter SW, Choi AM. Carbon monoxide confers protection in sepsis by enhancing beclin 1-dependent autophagy and phagocytosis. *Antioxid Redox Signal*. 2014;20:432–442. doi: 10.1089/ars.2013.5368
35. Bishop CA, Schulze MB, Klaus S, Weitkunat K. The branched-chain amino acids valine and leucine have differential effects on hepatic lipid metabolism. *FASEB J*. 2020;34:9727–9739. doi: 10.1096/fj.202000195R
36. Crown SB, Marze N, Antoniewicz MR. Catabolism of branched chain amino acids contributes significantly to synthesis of odd-chain and even-chain fatty acids in 3T3-L1 adipocytes. *PLoS One*. 2015;10:e0145850. doi: 10.1371/journal.pone.0145850
37. Lahiri V, Hawkins WD, Klionsky DJ. Watch what you (self-) eat: autophagic mechanisms that modulate metabolism. *Cell Metab*. 2019;29:803–826. doi: 10.1016/j.cmet.2019.03.003
38. Saito T, Kuma A, Sugiura Y, Ichimura Y, Obata M, Kitamura H, Okuda S, Lee HC, Ikeda K, Kanegae Y, et al. Autophagy regulates lipid metabolism through selective turnover of NCoR1. *Nat Commun*. 2019;10:1567. doi: 10.1038/s41467-019-08829-3
39. Lee I, Huttemann M. Energy crisis: the role of oxidative phosphorylation in acute inflammation and sepsis. *Biochim Biophys Acta*. 2014;1842:1579–1586. doi: 10.1016/j.bbadis.2014.05.031
40. Englert JA, Rogers AJ. Metabolism, metabolomics, and nutritional support of patients with sepsis. *Clin Chest Med*. 2016;37:321–331. doi: 10.1016/j.ccm.2016.01.011
41. Levine B, Klionsky DJ. Development by self-digestion: molecular mechanisms and biological functions of autophagy. *Dev Cell*. 2004;6:463–477. doi: 10.1016/S1534-5807(04)00099-1

42. Starr ME, Saito H. Sepsis in old age: review of human and animal studies. *Aging Dis*. 2014;5:126–136. doi: 10.14336/AD.2014.0500126
43. Shirakabe A, Ikeda Y, Sciarretta S, Zablocki DK, Sadoshima J. Aging and autophagy in the heart. *Circ Res*. 2016;118:1563–1576. doi: 10.1161/CIRCRESAHA.116.307474
44. Aman Y, Schmauck-Medina T, Hansen M, Morimoto RI, Simon AK, Bjedov I, Palikaras K, Simonsen A, Johansen T, Tavernarakis N, et al. Autophagy in healthy aging and disease. *Nat Aging*. 2021;1:634–650. doi: 10.1038/s43587-021-00098-4
45. Cabreiro F, Au C, Leung KY, Vergara-Irigaray N, Cocheme HM, Noori T, Weinkove D, Schuster E, Greene ND, Gems D. Metformin retards aging in *C. elegans* by altering microbial folate and methionine metabolism. *Cell*. 2013;153:228–239. doi: 10.1016/j.cell.2013.02.035
46. Ha J, Guan KL, Kim J. AMPK and autophagy in glucose/glycogen metabolism. *Mol Aspects Med*. 2015;46:46–62. doi: 10.1016/j.mam.2015.08.002
47. Adeva-Andany MM, Gonzalez-Lucan M, Donapetry-Garcia C, Fernandez-Fernandez C, Ameneiros-Rodriguez E. Glycogen metabolism in humans. *BBA Clin*. 2016;5:85–100. doi: 10.1016/j.bbacli.2016.02.001
48. Singh R, Kaushik S, Wang Y, Xiang Y, Novak I, Komatsu M, Tanaka K, Cuervo AM, Czaja MJ. Autophagy regulates lipid metabolism. *Nature*. 2009;458:1131–1135. doi: 10.1038/nature07976
49. Kaushik S, Cuervo AM. Degradation of lipid droplet-associated proteins by chaperone-mediated autophagy facilitates lipolysis. *Nat Cell Biol*. 2015;17:759–770. doi: 10.1038/ncb3166
50. Kawane K, Motani K, Nagata S. DNA degradation and its defects. *Cold Spring Harb Perspect Biol*. 2014;6:a016394. doi: 10.1101/cshperspect.a016394
51. Houseley J, Tollervey D. The many pathways of RNA degradation. *Cell*. 2009;136:763–776. doi: 10.1016/j.cell.2009.01.019
52. Rossi MA, Celes MR, Prado CM, Saggioro FP. Myocardial structural changes in long-term human severe sepsis/septic shock may be responsible for cardiac dysfunction. *Shock*. 2007;27:10–18. doi: 10.1097/01.shk.0000235141.05528.47
53. Standage SW, Bennion BG, Knowles TO, Ledee DR, Portman MA, McGuire JK, Liles WC, Olson AK. PPARalpha augments heart function and cardiac fatty acid oxidation in early experimental polymicrobial sepsis. *Am J Physiol Heart Circ Physiol*. 2017;312:H239–H249. doi: 10.1152/ajpheart.00457.2016
54. Drosatos K. Fatty old hearts: role of cardiac lipotoxicity in age-related cardiomyopathy. *Pathobiol Aging Age Relat Dis*. 2016;6:32221. doi: 10.3402/pba.v6.32221
55. Wasyluk W, Zwolak A. Metabolic alterations in sepsis. *J Clin Med*. 2021;10:2412. doi: 10.3390/jcm10112412
56. Chew MS, Shekar K, Brand BA, Norin C, Barnett AG. Depletion of myocardial glucose is observed during endotoxemic but not hemorrhagic shock in a porcine Pmodel. *Crit Care*. 2013;17:R164. doi: 10.1186/cc12843
57. Irahara T, Sato N, Otake K, Matsumura S, Inoue K, Ishihara K, Fushiki T, Yokota H. Alterations in energy substrate metabolism in mice with different degrees of sepsis. *J Surg Res*. 2018;227:44–51. doi: 10.1016/j.jss.2018.01.021
58. Douglas JJ, Walley KR. Metabolic changes in cardiomyocytes during sepsis. *Crit Care*. 2013;17:186. doi: 10.1186/1364-8535-17-186

SUPPLEMENTAL MATERIAL

Data S1. Evaluation of data quality, exploratory analysis, and data preprocessing

To remove the systematic variation between samples, we performed a median normalization such that all the samples have the same median value post log2 transformation. Below are box plots of before and after normalization.

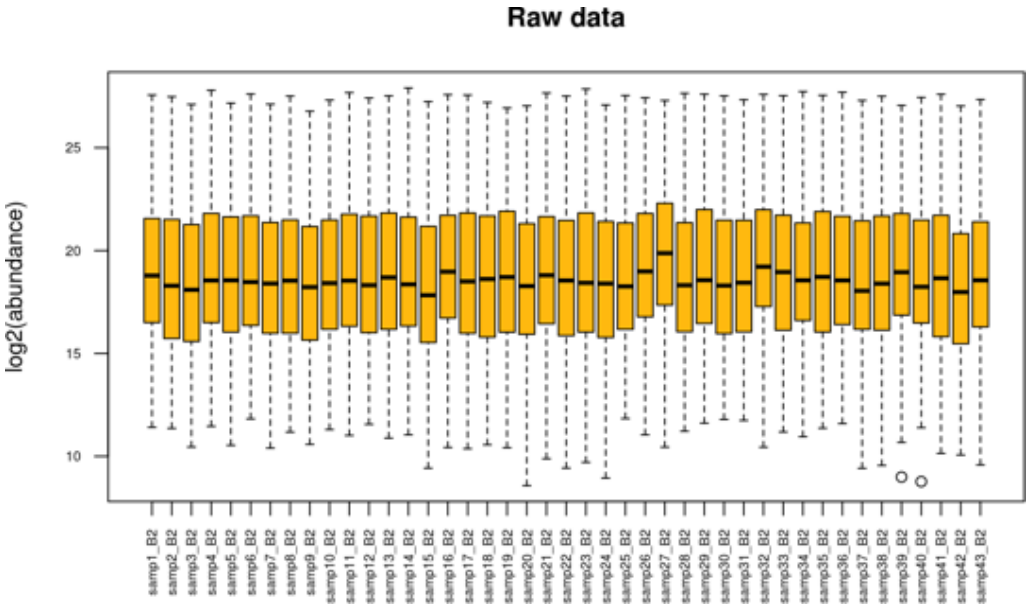

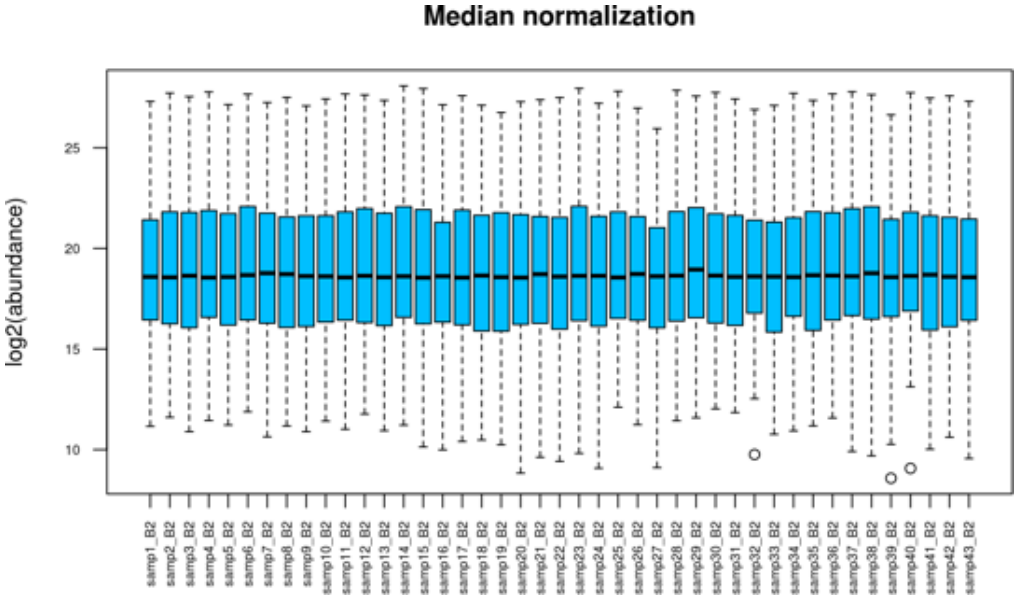

1) Date Filtering

This project used a targeted Mass Spec analysis designed to detect 361 metabolites. 199 of these metabolites were not detected in any of the samples and, therefore, had 100% missingness. The overall missingness of the remaining 162 metabolites was 1.2%. The figure below shows the percent missingness versus the mean log2-abundance for each metabolite.

We selected 156 metabolites with missingness < 20% and a coefficient of variation (CV) < 20% in the pooled sample QC data. After filtering, no missing values remained, therefore, no imputation was performed.

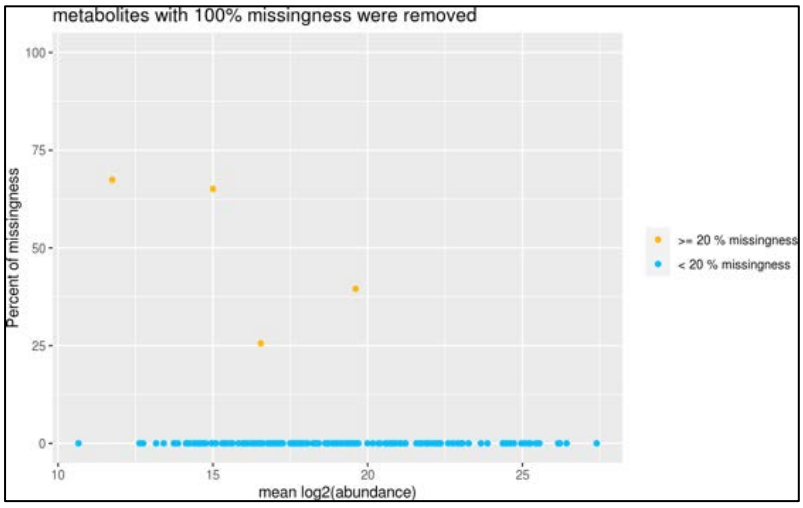

2) Evaluation of data quality-principal components analysis (PCA)

PCA is a method to take high dimensional data and reduce it to only a few dimensions to visualize how similar samples of the same type are. A series of PCA plots was generated using the log2 transformed, normalized, and filtered data. Potential variations driven by protein amount or run order were not observed detected.